A Stochastic Life Cycle and Greenhouse Gas Abatement Cost Assessment of Renewable Drop-in Fuels

by

Uyiosa Mark Oriakhi

B.Eng., Covenant University (2015)

Submitted to the Institute for Data, Systems, and Society
and the Department of Aeronautics and Astronautics
in partial fulfillment of the requirements for the degrees of

Master of Science in Technology and Policy

and

Master of Science in Aeronautics and Astronautics

at the

MASSACHUSETTS INSTITUTE OF TECHNOLOGY

February 2020

Signature redacted

Author .....
Institute for Data, Systems, and Society
and the Department of Aeronautics and Astronautics
January 17, 2020

Signature redacted

Certified by ....
Steven R. H. Barrett
Associate Professor of Aeronautics and Astronautics
Thesis Supervisor

Signature redacted

Accepted by ....
Noelle E. Selin
Director, Technology and Policy Program
Associate Professor, Institute for Data, Systems, and Society and
Department of Earth, Atmospheric, and Planetary Sciences

Acknowledgments

I want to thank my family: my parents for all the love and the uncountable sacrifices they have made, and my brothers: Tose, Osasu, and Zuwa, for being genuinely good people and making a great support system from the day I was born. This thesis isn't just for me - it's for all six of us.

I would also like to thank Dr. Mark Staples, who guided and oversaw my work from my first day at the LAE. I greatly appreciate everything, especially the effort in continuing to review this work after you left the lab.

Another person who has been of great help to me is Matthew Pearlson, who offered me counsel, advice, and motivation during the most challenging times in the process of producing this work. I am indeed very grateful.

Thanks also to Juju Wang, whose assistance and collaboration helped make this thesis possible; I appreciate everything.

I also want to thank my advisor, Prof. Steven Barrett, and the entire LAE for all the amazing work you do towards making aviation more sustainable - it's been an inspiration to me.

Finally, I want to thank the almighty God, my father in heaven, for the protection, the wisdom, and the unfathomable blessings all through my time at MIT, and indeed all through my life.

Contents

List of Figures

List of Tables

Chapter 1

Introduction

1.1 Background and Motivation

Emissions from commercial aircraft currently constitute approximately 2.6% of annual global carbon dioxide (CO_2) emissions from fossil fuel combustion [1], and 3.5% of total anthropogenic radiative forcing [2]. Commercial aviation is projected to increase by 4.3% every year for the next 20 years, largely due to lower ticket prices and the increase in economic activity in China, Southeast Asia, and the Middle East [1]. This increase in international aviation activity will likely lead to an even larger contribution to global anthropogenic climate change if the appropriate emissions reduction strategies are not adopted. In line with this, several bodies have set targets and established policies to reduce the climate impact of aviation. For example, the International Air Transport Association (IATA) has set a target of 50% reduction in net emissions by 2050 compared to 2005 levels [3]. Likewise, the International Civil Aviation Organization (ICAO), a specialized agency of the United Nations, has set a goal of carbon-neutral growth of international aviation from 2020 [4]. Members of ICAO's Committee on Aviation Environmental Protection (CAEP) have decided to adopt a market-based approach to facilitate reduction of international aviation emissions [5]. This initiative is called the Carbon Offsetting and Reduction Scheme for International Aviation (CORSIA). Under CORSIA, the average CO_2 emissions from international aviation between

2019 and 2020 will serve as a baseline to which all emissions from 2021 will be compared, and emissions above this baseline will be required to be offset by the international airlines [6]. The industry is also seeking ways to reduce CO_2 emissions through technological improvements such as the use of more fuel-efficient engines and operational improvements [7]. But these measures may not achieve the desired level of emissions reduction [7], which is why renewable drop-in fuels produced from biomass have received attention from policy makers as a means of significantly reducing aviation's carbon footprint [1].

Studies have been undertaken to ascertain the amount of greenhouse gas (GHG) emissions along the production life cycle of these renewable fuels. As illustrated in the diagram below, several of these studies have produced deterministic estimates under single or multiple scenarios. The wide range of values in the studies with multiple scenarios shows that there exists significant uncertainty in the life cycle GHG emissions of renewable drop-in fuels. But these results do not adequately capture the variance and the relative likelihood of different values within the indicated ranges. This is the problem that this study aims to address through a rigorous probabilistic quantification of the CO_2e (CO_2 equivalent) life cycle emissions of renewable drop-in aviation fuels. It is important to note that only CO_2, N_2O, and CH_4 emissions are included in this assessment, and the N_2O and CH_4 emissions are converted to CO_2e by multiplying by the appropriate 100-year Global Warming Potential (GWP).

Table 1.1: Deterministic LCA results in gCO_2e/MJ from previous studies for the pathways assessed

	Low	**Baseline**	**High**
Corn ATJ [8]	47.6	62.6	117.5
Sugarcane SIP [8]	-27.0	12.7	117.5
HEFA PFAD [9]		13.0	
HEFA FOG (Tallow) [10]	25.7		37.5
HEFA FOG (Yellow grease) [10]	16.8		21.4
Micro FT fuel from forest residue [11]		89.0	
FT fuel from municipal solid waste [12]		40.0	

There are six renewable fuel pathways considered in this study: jet fuel from the advanced

fermentation of corn via isobutanol, synthetic iso-paraffinic (SIP) kerosene from sugarcane, hydroprocessed esters and fatty acids (HEFA) from fats, oil, and greases, HEFA from palm fatty acids distillates, Fischer-Tropsch (FT) jet fuel from municipal solid waste, and micro FT jet fuel from forest residue. These renewable fuels have been certified by the American Society for Testing and Materials (ASTM) International [13]. The corn ATJ and sugarcane SIP pathways which use a commercial crop for feedstock are more mature and have been produced at a larger scale than the waste and residue pathways. Finally, the GHG abatement costs, which are the costs of reducing CO_2e emissions by one metric ton through the use of renewable fuel, are calculated by combining stochastic life cycle assessment (LCA) and stochastic techno-economic analysis (TEA). This stochastic abatement cost assessment is important because it enables us to compare the cost-effectiveness of the various pathways. It also provides a basis to compare the costs of these pathways with the costs of other climate change mitigation options and technologies. It should be noted, however, that the stochastic TEA was not developed by this thesis work, hence it will not be discussed in detail.

Chapter 2

Materials and Methods

2.1 Life Cycle Assessment

GHG Emissions arise during the cultivation, harvesting, transportation and conversion of the feedstocks used to produce renewable fuels, in addition to the emissions from combustion of the fuels [14]. Therefore, in order to properly assess the climate benefit of using these fuels, the emissions from all these stages must be properly accounted for, and this accounting process is known as life cycle assessment (LCA) [14]. For fuels produced from biogenic sources, the CO_2e emissions from combustion are typically not included in LCA. This is because combustion CO_2e emissions are offset by the CO_2 photosynthesized by the plant during growth [10].

There are two categories of variables that contribute to life cycle CO_2e emissions: material inputs and yield ratios. The former includes factors of production such as electricity, natural gas, and fertilizers. While the latter encompasses parameters such as crop yield and feedstock-to-fuel conversion ratio. These ratios are crucial to LCA because they determine the amounts of the physical inputs that are required to produce 1 MJ of the fuel. In cases where there are multiple products in one or more of the stages of the life cycle, the emissions are allocated to the product that is relevant to the jet fuel production life cycle. For example,

in the production of jet fuel from corn grain via isobutanol, GHG emissions are allocated between isobutanol and its co-product, distillers' grains and solubles (DGS). There are three bases on which these allocations are commomly carried out: energy, market value, and displacement. In this study, allocations were primarily done on an energy basis, following this formula:

$$\mathrm{AF}_x = \frac{\mathrm{L}_x \mathrm{M}_x}{\sum_{n=1}^{N} \mathrm{L}_n \mathrm{M}_n} \tag{2.1}$$

where:

AF_x is the allocation factor of co-product x,

L_x is the lower calorific value of co-product x,

M_x is the mass of co-product x,

L_n is the lower calorific value of co-product n,

M_n is the mass of co-product n,

N is the total number of co-products.

Upon completion of the LCA, an indicator of the environmental benefit of the renewable fuel is determined by comparing the life cycle CO_2e emissions value to the baseline value of 89.0 gCO_2e/MJ for conventional jet fuel [12].

2.2 Stochastic Life Cycle Assessment

The stochastic life cycle assessment (LCA) is a modified approach to the standard deterministic LCA described above. This approach involves quantifying the inherent uncertainty in the life cycle emissions of renewable drop-in fuels. This uncertainty arises from the variation in some of the parameters of production along the life cycle which contribute to CO_2e emissions. The stochastic LCA workflow begins with modeling of the processes involved in the life cycle and the identification of parameters to be treated as stochastic. After this, for each

of these parameters, data is collected and the known probability density function (PDF) that best fits the data is assigned to that variable. Once these distributions have been defined, a Monte Carlo simulation is carried out where values are drawn randomly from each of the distributions. These values, weighted by the appropriate emissions factors, are combined with the deterministic parameter values to generate the total life cycle emissions for each run of the Monte Carlo simulation. In this study, 10,000 Monte Carlo draws are made.

Parameters were treated as stochastic if they met three conditions: non-trivial impact on life cycle emissions, availability of data, and considerable variance in this data. Based on this approach, some physical inputs such as electricity, natural gas, fertilizers, and hydrogen were treated as stochastic variables in all pathways. Crop yields and feedstock-to-fuel conversion ratios were also treated as stochastic. Some other parameters were treated as deterministic and assigned constant values as opposed to probability density functions. For example, the emissions indices for the physical inputs were based on the deterministic values from the Greenhouse Gases, Regulated Emissions, and Energy Use in Transportation (GREET) software [11], and are given in Appendix B. The 100-year Global Warming Potentials (GWP) of N_2O and CH_4, 265 and 28 respectively, were also treated as deterministic and obtained from GREET [11].

This study does not include emissions from one-time processes such as the construction of the fuel production plant; it only includes on-going, operational emissions in the fuel life cycle. This is because these one-time emissions were found to be minute when compared to the total emissions over the time period after the initial establishment of the facility. The penultimate life cycle stage, fuel transportation and distribution (T & D), is also not included as it typically contributes less than 0.1% to the total life cycle CO_2e emissions [10]. Finally, the system boundaries considered in this study do not include land use change (LUC).

In the following sections, the stochastic life cycle assessments for the six renewable fuel pathways are discussed. These discussions cover the data sources, assumptions, life cycle scope, and the probability density functions which were assigned to the respective parame-

ters. For descriptions of the fuel production technologies, refer to Appendix A.

2.2.1 Corn Alcohol-to-Jet (ATJ)

The first pathway considered was the production of jet fuel from corn via isobutanol. The system boundary, which is the set of stages considered in the LCA, included all stages from feedstock cultivation to the upgrading of the alcohol to jet fuel. These are: feedstock cultivation, transportation to the facility, fermentation to alcohol, and the upgrading from alcohol to jet fuel.

Corn yield data from the United States Department of Agriculture (USDA) [15] was analyzed. It was fit to Gaussian, Weibull, and Beta distributions, and the Weibull distribution produced the best fit of the data. Data for limestone, nitrogen (N), phosphorus (P), and potassium (K) fertilizer usage was also obtained from the USDA report on the 2008 energy balance for the corn-ethanol industry [16], while herbicide application data was from Wang et al. (2012) [17]. Uniform and Triangular disributions were compared for the N, P, and K fertilizers. Data were evenly distributed throughout the range and not concentrated at any point, hence the uniform distribution was assigned with limits being the lowest and highest values in data after the removal of outliers. The limestone was assigned a Weibull PDF, and a triangular distribution was assigned to the herbicides. The Weibull PDF for the energy usage of the farm machinery was obtained from Wang et al. [17] and the share: diesel (49%), liquefied petroleum gas (18%), gasoline (15%), natural gas (13%), and electricity (5%) was obtained from the Greenhouse gases, Regulated Emissions, and Energy use in Transportation Model (GREET) software [11]. The transportation emissions data was obtained from the 2017 ICF international inc. life cycle analysis of corn-based ethanol [18]. The probability distributions for feedstock-to-fuel ratio and the utility requirements in the fermentation stage were obtained from Staples et al. [8]. The distributions for the energy usage in the upgrading stage were also obtained from Staples et al. [8]. It should also be noted that the fermentation process yields two products: isobutanol and distiller's grains and solubles

(DGS). Therefore, the emissions attributable to fermentation and all stages upstream were allocated between these two products on an energy basis.

Table 2.1: Probability density functions for stochastic variables in the corn AJF pathway (Uniform [low, high], Triangular (low, mode, high), Weibull (scale, shape))

Stage	Parameter	Distribution	Unit
Cultivation	N Fertilizer [16]	Uniform [44.45, 78.47]	kg/acre
	P Fertilizer [16]	Uniform [14.97, 42.18]	kg/acre
	K Fertilizer [16]	Uniform [8.68, 51.71]	kg/acre
	Herbicides [17]	Triangular (0.89, 1.18, 1.28)	kg/acre
	Limestone [15]	Weibull (778.4, 10.0)	lbs/acre
	Energy [17]	Weibull (416.4, 6.3)	$MJ/tonne_{corn}$
	Corn yield [15]	Weibull (188,9, 6.7)	bushel/acre
Feedstock transportation	CO_2e Emissions [16]	Uniform [111.57, 161.67]	gCO_2e/bushel
Fermentation	Hydrogen [8]	Triangular (0.333, 0.334, 0.335)	g/MJ_{fuel}
	Electricity [8]	Triangular (0.071 0.076, 0.084)	MJ/MJ_{fuel}
	Natural gas [8]	Triangular (0.367, 0.389, 0.426)	MJ/MJ_{fuel}
Upgrading	Electricity [8]	Uniform [0.015, 0.026]	MJ/MJ_{fuel}
	Natural gas [8]	Uniform [0.179, 0.339]	MJ/MJ_{fuel}
	Feedstock-to-fuel ratio [8]	Triangular (0.0050 0.0054, 0.0059)	$bushel/MJ_{fuel}$

2.2.2 Synthetic Iso-Paraffinic (SIP) Kerosene from Sugarcane

Another renewable drop-in fuel produced from a commodity crop was considered in this study: synthetic iso-paraffinic (SIP) kerosene using sugarcane as feedstock. As in the corn AJF pathway, the system boundary begins at the cultivation stage and ends at the fuel production stage. The data for the N, P, and K fertilizer inputs on the farm were obtained from the Food and Agriculture Organization of the United Nations (FAO) [19]. From the analysis of this data, triangular distributions were assigned to N and K fertilizers, while the P fertilizer was deemed to follow a uniform distribution. The crop yield data obtained from the Sugarcane Industry Union (UNICA) [20] was tested with different probability distribution functions and the Weibull distribution gave the best fit. The data for limestone and farm energy inputs were obtained from the GREET software and were both assigned a triangular PDF. The share of the energy for farming was based on information from GREET and is as follows: diesel (38%), liquefied petroleum gas (19%), gasoline (12%), natural gas (22%), and electricity (9%). The feedstock-to-fuel conversion ratio was deemed to follow a triangular

distribution based on work done by Staples et al. [8]. Finally, the CO_2e emissions from feedstock transportation were assigned a uniform PDF based on data from GREET [11]. There are three products from sugarcane: sugars, which are used in the SIP process, and two co-products: molasses and bagasse. Therefore, as it is the corn ATJ pathway, farming emissions were allocated between these products on an energy basis. And crucially, the energy derived from the sugarcane bagasse satisfies all the energy requirements in the fuel production stage through co-generation. Hence, all emissions in this process are considered biogenic and no emissions are attributed to it, as shown in table 2.2.

Table 2.2: Probability density functions for stochastic variables in the sugarcane SIP pathway (Uniform [Low, High], Triangular (Low, Mode, High), Weibull (scale, shape), Normal (mean, standard deviation))

Stage	**Parameter**	**Distribution**	**Unit**
Cultivation	N Fertilizer [19]	Triangular (14, 59, 76)	kg/ha
	P Fertilizer [19]	Uniform [28, 60]	kg/ha
	K Fertilizer [19]	Triangular (63, 113, 130)	kg/ha
	Limestone [11]	Triangular (4836, 5200, 5468)	kg/ha
	Energy [11]	Triangular (82, 100, 111.6)	MJ/ha
	Crop yield [20]	Weibull (27, 8.162)	tonne/acre
	Feedstock-to-fuel ratio [8]	Triangular (0.646, 0.996, 1.531)	kg/MJ_{fuel}
Feedstock transportation	CO_2e Emissions [11]	Uniform [13.90, 17.70]	gCO_2e/bushel

2.2.3 Hydroprocessed Esters & Fatty Acids (HEFA) from Palm Fatty Acid Distillates (PFAD)

The third pathway considered was that of jet fuel produced from palm fatty acids distillates (PFAD) through the HEFA process. PFAD is a by-product of palm oil refining which could be considered as a waste product or as a valuable resource. If deemed the former, then the system boundary would not include the cultivation and palm oil milling stages – only the feedstock transportation and HEFA process. In this study, assessments were carried out for both cases: PFAD as a waste product (System boundary I), and PFAD as a valuable material (System boundary II). The crop yield data was obtained from palmoilanalytics.com [21] and was assigned a Gaussian distribution. The N, P, and K fertilizers were each deemed to

follow a uniform distribution based on analysis of the fertilizer usage data from Harsono et al. [22] Also, the diesel used by the farm machinery and the steam and electricity for the palm oil milling process were each assigned triangular distributions after data from Harsono et al. [22] was analyzed. A uniform distribution was chosen to represent the diesel used in transportation to the plant based on data from Jannick [23], and the fuel yield was assigned a Beta distribution based on Seber at al. [10] The Beta distribution gives a normalized representation of the variable, and hence was scaled up by the appropriate factor, in this case a factor of 303.8. Lastly, the hydrogen, electricity, and natural gas utilized in the HEFA process were each deemed to follow a triangular distribution [10]. As PFAD is not the only product of the fresh fruit brunches harvested, the emissions from the cultivation and the palm oil milling stages were necessarily allocated between PFAD and the other products. Following the same convention as in the previous two pathways, the allocation was on the basis of energy content.

Table 2.3: Probability density functions for stochastic variables in the HEFA PFAD pathway (Uniform [low, high], Triangular (low, mode, high), Weibull (scale, shape), Beta (α, β))

Stage	**Parameter**	**Distribution**	**Unit**
Cultivation	N Fertilizer [22]	Uniform [37, 53]	kg/ha
	P Fertilizer [22]	Uniform [91, 114]	kg/ha
	K Fertilizer [22]	Uniform [77, 110]	kg/ha
	Diesel [23]	Triangular (1951, 2038, 2366)	MJ/ha
	Crop yield [21]	Normal (5.126, 0.759)	tonne/ha
Palm oil milling	Electricity [22]	Triangular (0.42, 0.69, 0.78)	GJ/ha
	Steam [22]	Triangular (18.51, 30.34, 34.66)	GJ/ha
Feedstock transportation	Diesel [22]	Uniform [1.10, 1.95]	GJ/ha
HEFA Process	Electricity [10]	Triangular (2.86, 6.80, 11.34)	$\text{MJ}/100\text{lb}_{\text{PFAD}}$
	Natural gas [10]	Triangular (13.15, 66.23, 101.61)	$\text{MJ}/100\text{lb}_{\text{PFAD}}$
	Hydrogen [10]	Triangular (0.0013, 0.0023, 0.0032)	$\text{lb}/\text{MJ}_{\text{fuel}}$
	Fuel yield [10]	Beta (4.8, 1.2)[a]	$\text{GGE}/\text{tonne}_{\text{PFAD}}$

[a]The domain of the Beta distribution is $[0, 1]$, hence it gives a normalized representation of the parameter. To obtain the parameter value used for computations, the normalized value was scaled up by the appropriate factor of 303.8.

2.2.4 HEFA from Fats, Oils, and Greases (FOG)

The HEFA process utilizing fats, oils, and greases (FOG) as feedstock was also considered. These FOGs are of two kinds: beef tallow feedstock and used cooking oil (yellow grease) feedstock. The process of converting fats, oils, and greases to jet fuel through HEFA includes three stages: rendering, transportation to the plant, and the HEFA process. For yellow grease, the transportation emissions and the utility requirements for the rendering stage were assigned a triangular distribution based on the data analyzed from Seber et al. [10] The parameters for the HEFA process and the fuel yield are the same as those for the HEFA PFAD pathway.

Table 2.4: Probability density functions for stochastic variables in the HEFA FOG (Yellow grease) pathway (Uniform [low, high], Triangular (low, mode, high), Weibull (scale, shape), Beta (α, β))

Stage	Parameter	Distribution	Unit
Rendering	Electricity [10]	Triangular (0.06, 0.15, 0.25)	MJ/kg_{FOG}
	Natural gas [10]	Triangular (0.29, 1.46, 2.24)	MJ/kg_{FOG}
Feedstock transportation	CO_2e emissions [10]	Uniform [0.60, 0.84]	gCO_2e/MJ_{fuel}
HEFA Process	Electricity [10]	Triangular (2.86, 6.80, 11.34)	$MJ/100\ lb_{FOG}$
	Natural gas [10]	Triangular (13.15, 66.23, 101.61)	$MJ/100\ lb_{FOG}$
	Hydrogen [10]	Triangular (0.0013, 0.0023, 0.0032)	lb/MJ_{fuel}
	Fuel yield [10]	Beta (4.8, 1.2)[b]	$GGE/tonne_{FOG}$

[b]The domain of the Beta distribution is $[0, 1]$, hence it gives a normalized representation of the parameter. To obtain the parameter value used for computations, the normalized value was scaled up by the appropriate factor of 303.8.

For beef tallow, the electricity used for rendering was assigned a uniform distribution based on data from Chen et al. [24]. For the transportation parameter, the uniform distribution was chosen for the emissions based on data from [10]. And like the yellow grease case, the parameters for the HEFA process and the fuel yield are the same as those for the HEFA PFAD pathway.

2.2.5 Micro Fischer-Tropsch Jet Fuel from Forest Residue

Jet fuel produced from forest residue through the micro Fischer-Tropsch process was another pathway assessed in this study. There are three stages in the life cycle: forest residue

Table 2.5: Probability density functions for stochastic variables in the HEFA FOG (Tallow) pathway (Uniform [low, high], Triangular (low, mode, high), Weibull (scale, shape), Beta (α, β))

Stage	Parameter	Distribution	Unit
Rendering	Electricity [24]	Uniform [0.380, 0.736]	MJ/lbs_{FOG}
	Natural gas [24]	Triangular (1.567, 3.409, 6.048)	MJ/lbs_{FOG}
Feedstock transportation	CO_2e emissions [10]	Uniform [0.60, 0.84]	gCO_2e/MJ_{fuel}
HEFA Process	Electricity [10]	Triangular (2.86, 6.80, 11.34)	$MJ/100\ lb_{FOG}$
	Natural gas [10]	Triangular (13.15, 66.23, 101.61)	$MJ/100\ lb_{FOG}$
	Hydrogen [10]	Triangular (0.0013, 0.0023, 0.0032)	lb/MJ_{fuel}
	Fuel yield [10]	Beta (4.8, 1.2)[c]	$GGE/tonne_{FOG}$

[c]The domain of the Beta distribution is $[0, 1]$, hence it gives a normalized representation of the parameter. To obtain the parameter value used for computations, the normalized value was scaled up by the appropriate factor of 303.8.

collection, forest residue transportation, and jet fuel production. For the collection stage, the GHG emissions realized from the machinery usage were deemed to follow a uniform distribution based on data from the GREET software [11]. For the transportation stage, the emissions attributable to the diesel used were assigned a triangular distribution after analysis of the data also from the GREET software [11]. Lastly, point estimates were used for the electric power for jet fuel production and the feedstock-to-fuel conversion ratio.

Table 2.6: Probability density functions for stochastic variables in the Micro FT jet fuel from forest residue pathway (Uniform [low, high], Triangular (low, mode, high))

Stage	Parameter	Distribution	Unit
Feedstock collection	CO_2e emissions [11]	Uniform [4.78, 6.33]	gCO_2e/MJ
Feedstock transportation	CO_2e emissions [11]	Triangular (8.23, 12.67, 16.45)	gCO_2e/MJ

2.2.6 Fischer-Tropsch Jet Fuel from Municipal Solid Waste (MSW)

The final pathway considered in this study was that of jet fuel produced from municipal solid waste through conventional gasification and Fischer-Tropsch synthesis. The feedstock utilized are the discards from MSW which had been sorted for recyclables and compost. It is important to note that this feedstock is not completely biogenic, as it contains non-biogenic materials such as plastics and rubber [25, 26]. Due to this, the CO_2e emissions from fuel combustion are not fully offset, hence the life cycle is analyzed from well-to-wake, unlike the

other pathways earlier discussed.

There are five stages considered in this LCA: feedstock collection, feedstock transportation, additional sorting of feedstock, jet fuel production, and jet fuel combustion. Note that there is a replaced waste management credit associated with the first stage. This is because the landfilling and incineration of MSW that would have occurred is avoided due to the MSW being utilized for fuel production [25]. From the work of Suresh [25] which drew from the Environmental Protection Agency (EPA) Waste Reduction Model (WARM) [27] and Penman et al. [28], this credit parameter was treated as stochastic and assigned a triangular distribution. The second step, feedstock transportation, had a triangular distribution assigned to it based on the work of Suresh [25]. There is also a recycling credit associated with the additional sorting step, and this parameter was also assigned a triangular distribution [25, 27, 29]. For the fuel production step, normal distributions were assigned to natural gas and petroleum coke [25, 30], while a triangular distribution was assigned to the utility requirements for MSW pre-processing [25] [31–33]. The fuel yield was deemed to be best described by a Beta PERT distribution [25] [31] [34–36], and the lower heating value of MSW was assigned a uniform distribution [25, 26] [37–40]. Finally, the CO_2e emissions from fuel combustion was assigned a triangular distribution [25, 41].

Table 2.7: Probability density functions for stochastic variables in the FT jet fuel from MSW pathway (Uniform [low, high], Triangular (low, mode, high), PERT (low, mode, High), Normal (mean, standard deviation)). Where MSW = Pre-processed MSW, PMSW = Processed MSW

Stage	Parameter	Distribution	Unit
Feedstock collection	Replaced waste management strategy credit [25] [27, 28]	Triangular (- 192.3, -167.2, -142.1)	$gCO_2e/tonne_{MSW}$
Feedstock transportation	CO_2e emissions [25]	Triangular (1.88, 3.76, 13.16)	gCO_2e/MJ_{fuel}
Additional sorting	Recycling credit [25] [27] [29]	Triangular (- 242.5, - 144.6, -77.2)	$gCO_2e/tonne_{MSW}$
Jet fuel production	Utility [25] [31–33]	Triangular (0.06, 0.13, 0.15)	MJ/kg_{MSW}
	Natural gas [25] [30]	Normal (6, 0.6)	g/kg_{PMSW}
	Petroleum coke [25] [30]	Normal (50, 5.0)	g/kg_{PMSW}
	Fuel yield [25] [31] [34–36]	PERT(49.70, 53.54, 57.16)	MJ/MJ_{MSW}
	LHV [25] [26] [37–40]	Uniform [19.99, 21.79]	MJ/kg_{MSW}
Jet fuel combustion	CO_2e emissions [25] [41]	Triangular (69.7, 71.7, 74.4)	gCO_2e/MJ_{fuel}

2.3 Abatement Cost Assessment

2.3.1 Stochastic Techno-Economic Analysis (TEA)

The techno-economic analysis for the jet fuel pathways involves the financial modeling of the processes and facilities required for fuel production. This analysis takes into account the various factors of production that contribute to the fixed and variable costs associated with the fuel production in the plant. Just like the stochastic LCA, the stochastic TEA probabilistically quantifies uncertainty – in this case, uncertainty associated with the costs of production of the fuel.

There are three types of uncertainty quantified in the stochastic TEA: technical uncertainty, fuel and utility price uncertainty, and policy uncertainty. It should be noted that in the TEA utilized in this study was under a "no policy" assumption for all pathways [42]. The stochastic TEA process includes n^{th} plant modeling [42], collection of data for the relevant parameters and fitting appropriate distributions to them [43]. Uniform distributions were selected in cases where there was little data, and beta PERT or triangular distributions were selected when there existed mode, minimum and maximum values of the variable [43]. The probability distributions were sampled from and used in a Monte Carlo simulation which outputs stochastic estimates for the minimum selling price (MSP) of the fuel, which is calculated using a Discounted Cash Flow Rate of Return (DCFROR) model.

2.3.2 Abatement Cost Calculation

The CO_2e abatement cost associated with a renewable fuel is the cost of reducing CO_2e emissions by 1 tonne through the replacement of conventional jet fuel with that fuel. The standard unit for this quantity is \$/tonne CO_2e and is calculated as:

$$\mathrm{A}_x = \frac{\mathrm{MSP}_x - \mathrm{P}_j}{\mathrm{E}_j - \mathrm{E}_x} \tag{2.2}$$

where:

A_x is the CO_2e abatement cost of renewable drop-in fuel x,

MSP_x is the minimum selling price of renewable drop-in fuel x,

P_j is the selling price of conventional jet fuel,

E_j is the life cycle CO_2e emissions of conventional jet fuel,

E_x is the life cycle CO_2e emissions of renewable drop-in fuel x.

For each pathway in this study, the stochastic LCA and TEA models were paired to calculate the abatement cost. This was done because there are several parameters such as natural gas, hydrogen and electricity used in the plant, which contribute directly to both CO_2e emissions and production costs. This ensures that we generate self-consistent CO_2e abatement cost estimates.

Chapter 3

Results and Discussion

3.1 Stochastic LCA Results

In the preceding sections, the motivation for the stochastic LCA was discussed and the methodology was outlined. In this section, the results of the Monte Carlo simulations with 10,000 random draws from each of the distributions defined in section 2.2 are analyzed. The statistical properties of the resulting distribution of life cycle emissions are noted, as well as the percentage responsibility from each stage of the life cycle.

3.1.1 Corn Alchohol-to-jet (ATJ)

The Monte Carlo simulation with 10,000 members yielded a mean value of 69.5 gCO_2e/MJ for the total emissions in the production life cycle of renewable jet fuel from corn via isobutanol. This represents a 23% reduction from the conventional jet fuel baseline emissions value of 89.0 gCO_2e/MJ [12]. 95% of the stochastic LCA results lie within 60.7 – 86.0 gCO_2e/MJ. The median value of 68.3 gCO_2e/MJ is lower than the mean, and the positive skewness value of 2.184 indicates that the distribution is right-skewed, which can be seen from the tail in the histogram. The standard deviation is 6.65 gCO_2e/MJ and the kurtosis is 14.82, cf. the kurtosis of the Normal distribution, which is 3. 34.7% of the emissions were

from the fertilizers, herbicides, limestone, and energy usage in the corn cultivation stage. Approximately 0.1% was from the diesel usage in the feedstock transportation stage. 43.7% was from the hydrogen, natural gas, and electricity usage in the fermentation stage, while 21.5% was from the electricity and natural gas usage in the upgrading of isobutanol to jet fuel. Finally, the mean value of 69.5 gCO_2e/MJ is 7.3% lower than the CORSIA determined life cycle value of 75 gCO_2e/MJ [12].

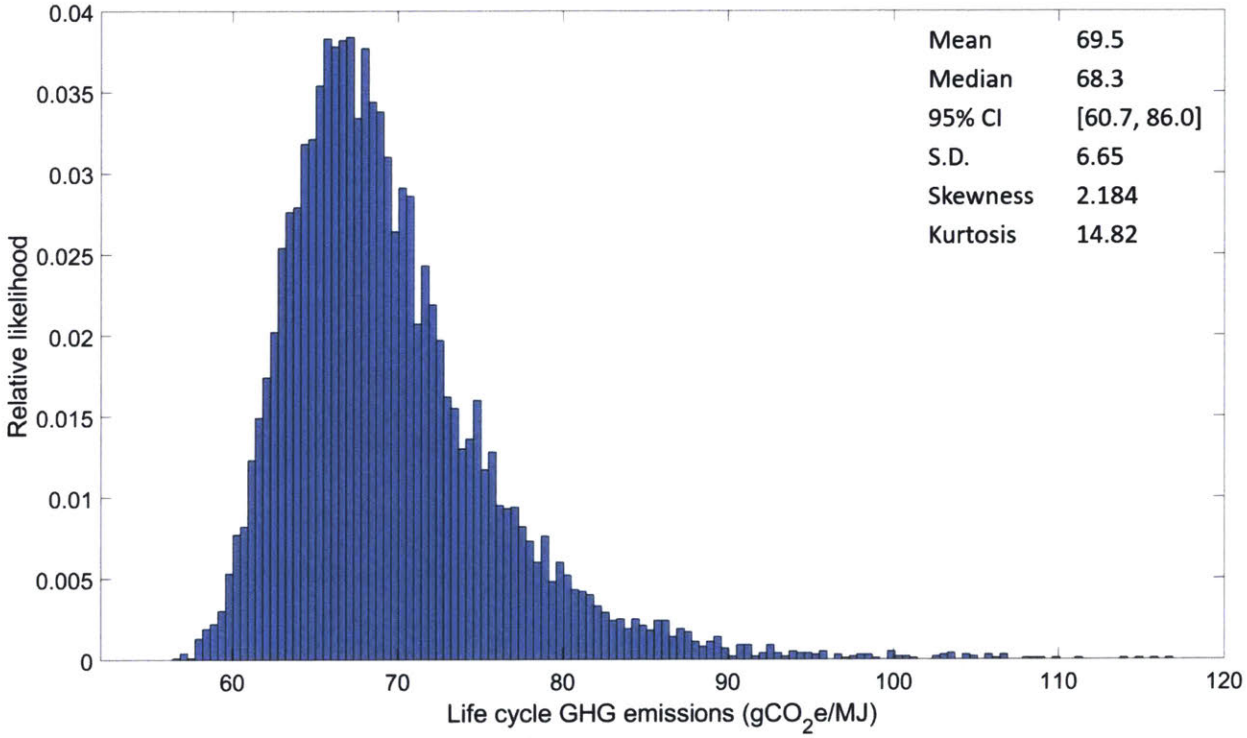

Figure 3-1: Monte Carlo simulation results for the corn ATJ LCA.

3.1.2 Sugarcane SIP

For the sugarcane SIP pathway, the mean value of total life cycle emissions was 35.1 gCO_2e/MJ. This represents a 61% reduction from the conventional jet fuel baseline emissions value of 89.0 gCO_2eq. 95% of the stochastic LCA results lie within 25.8 – 46.2 gCO_2e/MJ, with a median value of 34.7. The skewness value of 0.358 indicates that this is a right-skewed distribution. The standard deviation from the mean is 5.36 gCO_2e/MJ and the kurtosis value is 2.74. As mentioned in section 2.2.3, all emissions in this pathway are attributable to the

farming and feedstock transportation steps due to the self-sustaining nature of the downstream processes as a result of bagasse cogeneration. We find that 92.8% of the emissions are from the cultivation stage and 7.2% arise from feedstock transportation. Lastly, we note that the mean value of 35.1 gCO_2eq/MJ is 30.6% lower than the CORSIA determined life cycle value of 50.6 gCO_2e/MJ [12].

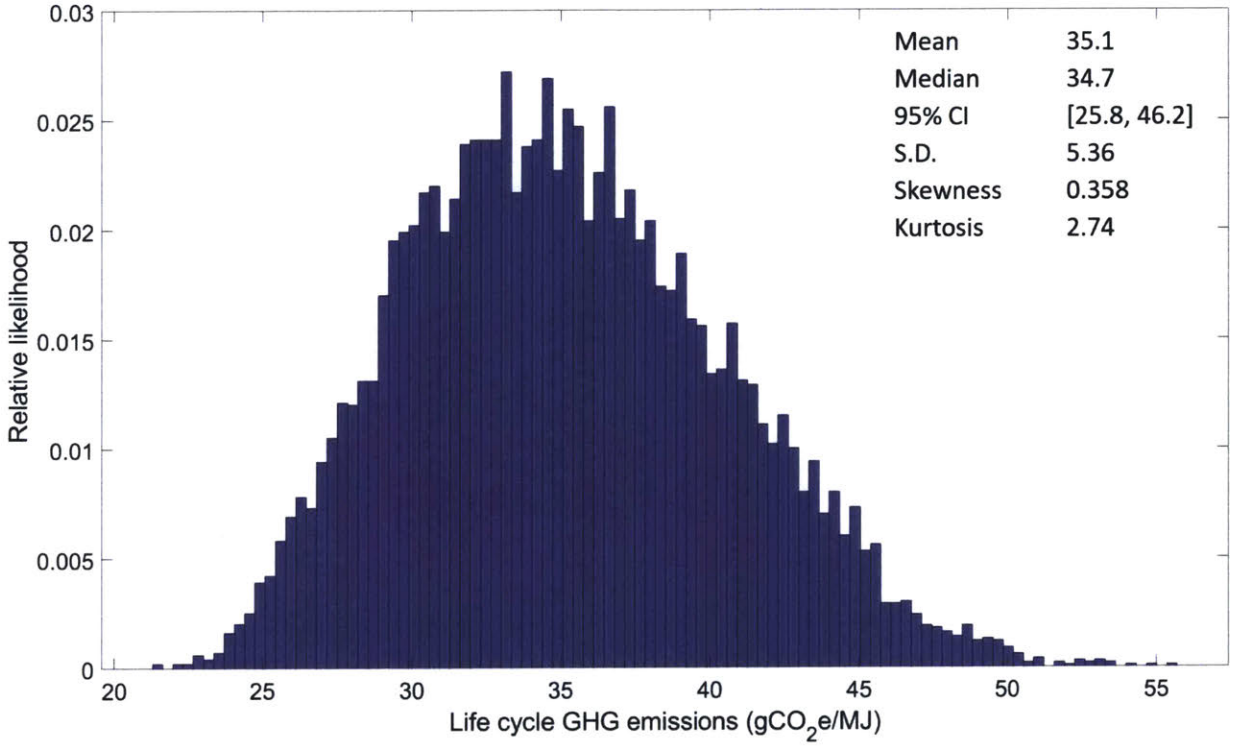

Figure 3-2: Monte Carlo simulation results for the sugarcane SIP LCA.

3.1.3 HEFA PFAD

We considered two system boundaries for the HEFA PFAD pathway: PFAD as a waste product (system boundary I) and PFAD as a valuable product (system boundary II). In the case of the former, the mean value of life cycle emissions was 20.7 gCO_2eq/MJ for the total life cycle emissions of corn ATJ. This represents a 77% reduction from the conventional jet fuel baseline emissions value of 89.0 gCO_2e/MJ. 95% of the stochastic LCA results lie within 14.9 – 26.5 gCO_2e/MJ, with a median value of 20.8gCO_2e/MJ. The standard deviation is 3.03

gCO_2e/MJ, the skewness is - 0.038, and the kurtosis is 2.64. As PFAD is treated as waste in this scenario, GHG emissions were attributed to only the feedstock transportation and the HEFA process. It was found that 0.1% of the emissions arise from the diesel combusted during feedstock transportation. Finally, the mean value of 20.7 gCO_2e/MJ is equal to the CORSIA life cycle emissions value for this pathway.

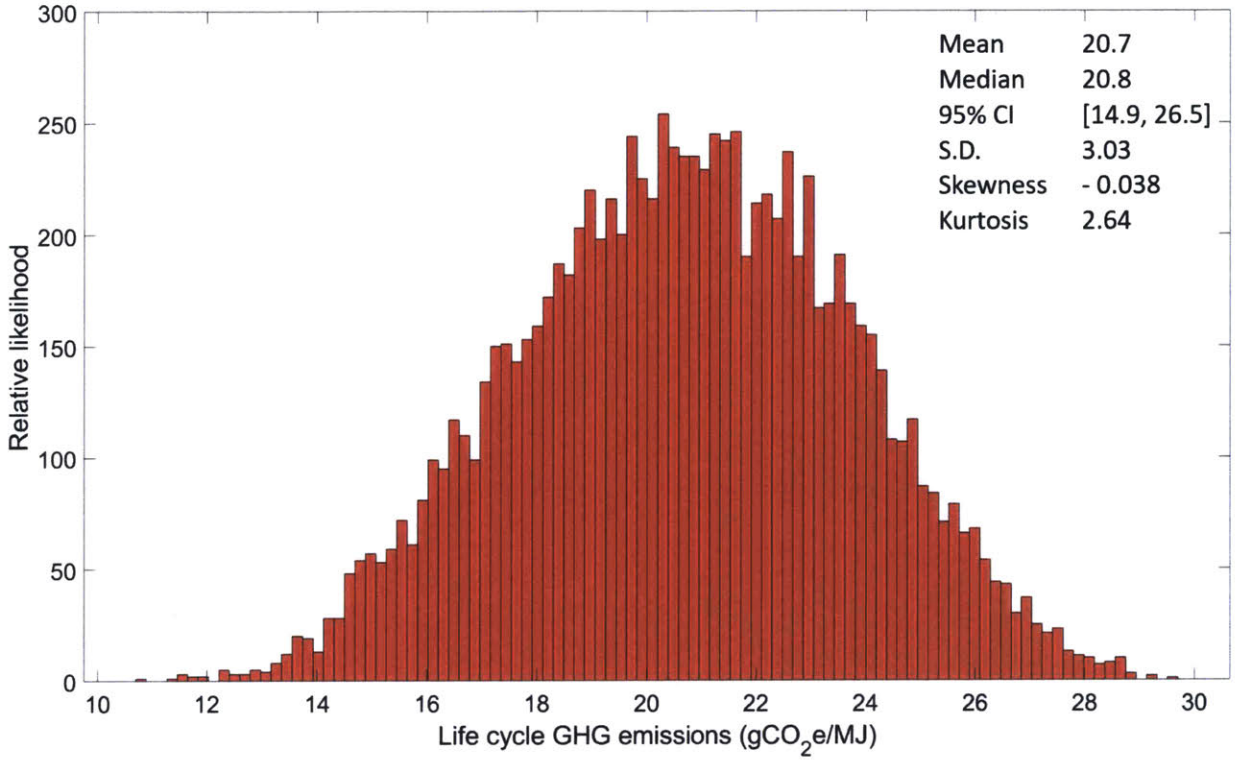

Figure 3-3: Monte Carlo simulation results for the HEFA PFAD LCA (System boundary I).

In system boundary II, the emissions from the upstream processes: cultivation and milling, add 1.9 gCO_2e/MJ to the total emissions from system boundary I. They respectively make up 3.2% and 5.1% of the emissions, while HEFA makes up 91.6% and only 0.1% is attributable feedstock transportation. The difference between the LCA value and that of CORSIA is now 10%, and emissions reduction from the conventional fuel baseline is 75%. Finally, the skewness value was found to be - 0.030, while the standard deviation and kurtosis differ from that of system boundary I by less than 1%.

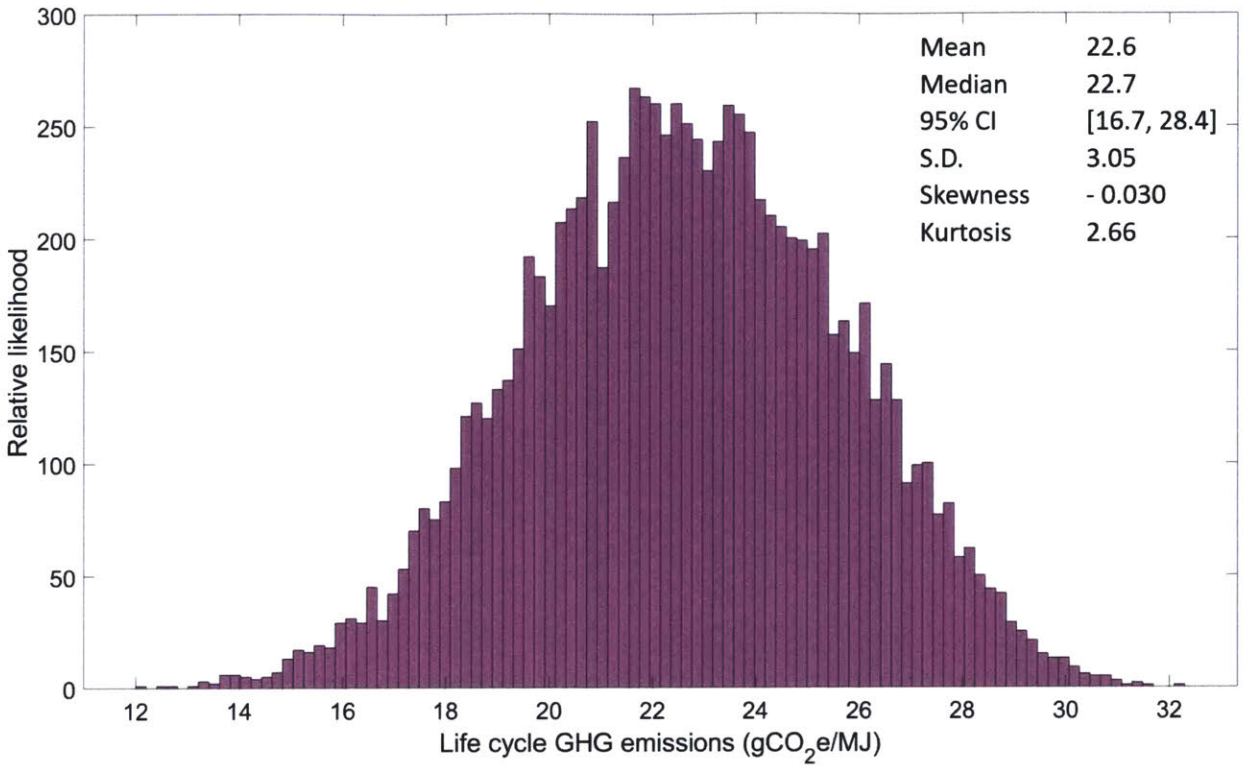

Figure 3-4: Monte Carlo simulation results for the HEFA PFAD LCA (System boundary II).

3.1.4 HEFA FOG (Yellow grease)

The stochastic LCA for the HEFA FOG (Yellow grease) pathway yielded a mean value of 24.5 gCO_2eq/MJ which translates to a 72% reduction in emissions compared to the conventional fuel baseline of 89.0 gCO_2eq/MJ. 95% of the values lie between 18.5 – 30.4 gCO_2e/MJ, while the median is equal to the mean. The standard deviation is 3.14 gCO_2eq/MJ, the skewness is - 0.032, and the kurtosis is 2.65. It was found that 12.5% of the emissions in this life cycle are from the beef tallow rendering process, 2.9% are from the transportation stage, while 84.6% are from the production of jet fuel. Lastly, we computed a mean value which is 9% higher than the CORSIA value of 22.5 gCO_2e/MJ.

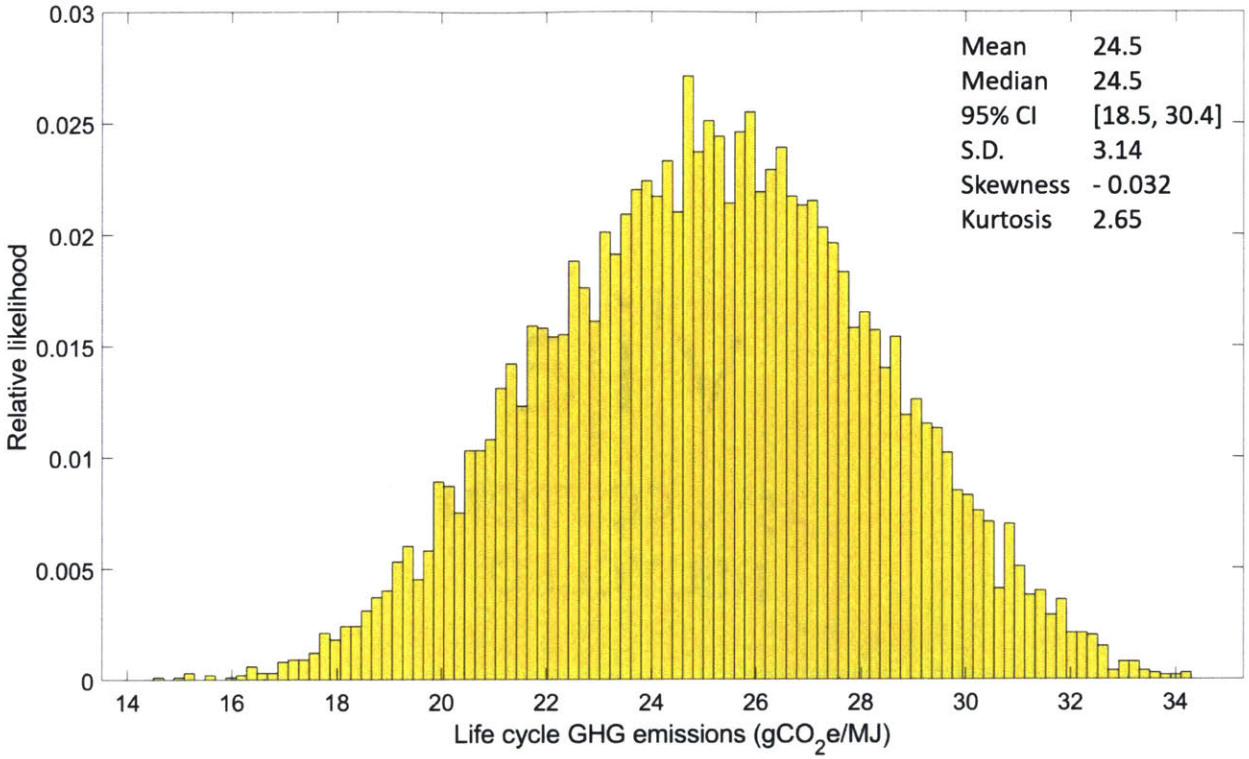

Figure 3-5: Monte Carlo simulation results for the HEFA FOG (Yellow grease) LCA.

3.1.5 HEFA FOG (Tallow)

The stochastic LCA for the HEFA FOG (Beef tallow) pathway yielded a mean value of 35.6 gCO_2eq/MJ which translates to a 60% reduction in emissions compared to the conventional fuel baseline of 89.0 gCO_2eq/MJ. 95% of the values lie between 27.5 – 43.8 gCO_2e/MJ, while the median value is 35.5 gCO_2e/MJ. The standard deviation was found to be 4.20 gCO_2eq/MJ, while the skewness is 0.028 and the kurtosis is 2.78. 39.5% of the emissions in this life cycle are from the beef tallow rendering process, 2.0% are from the diesel combustion during feedstock transportation, and 58.5% are attributable to the HEFA process. Lastly, we note that the mean value of 35.6 gCO_2e/MJ is 58% larger than the CORSIA value of 22.5 gCO_2e/MJ.

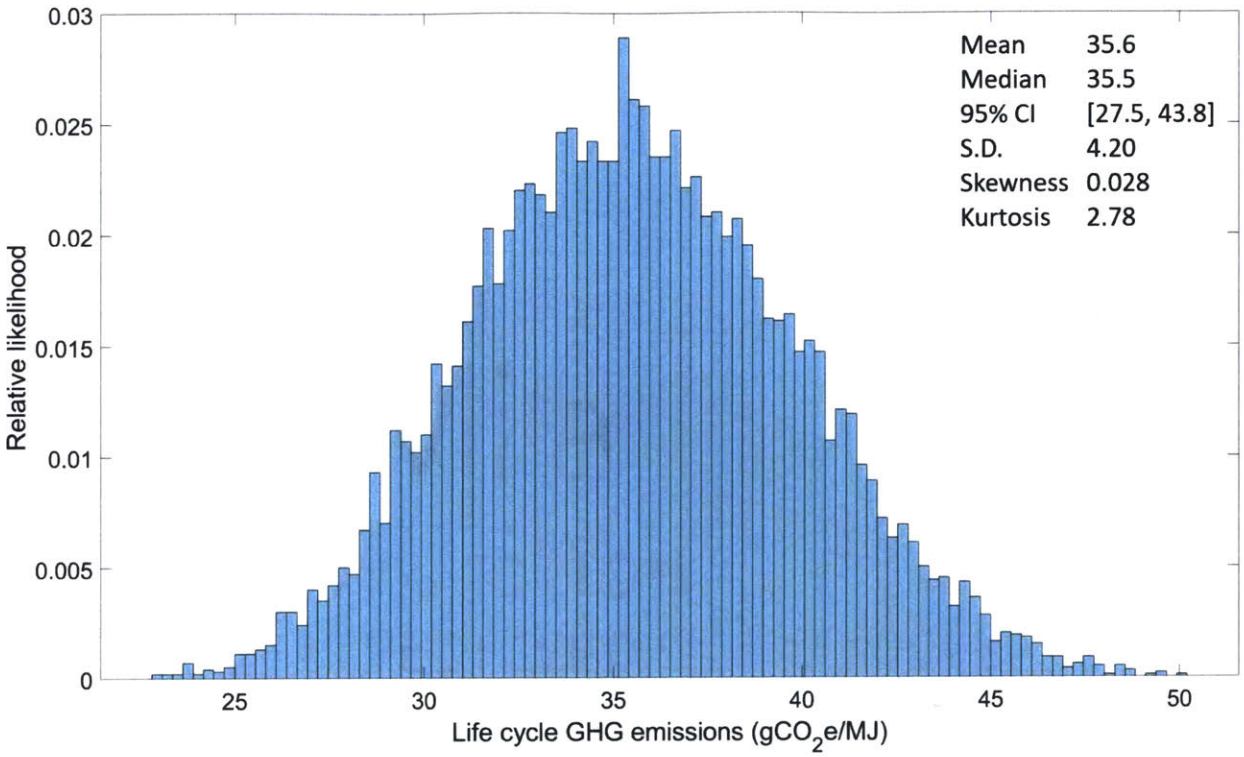

Figure 3-6: Monte Carlo simulation results for the HEFA FOG (Tallow) LCA.

3.1.6 Micro Fischer-Tropsch Jet Fuel from Forest Residue

The stochastic LCA for the Micro FT from forest residue pathway yielded a mean value of 41.3 gCO_2eq/MJ which translates to a 54% reduction in emissions compared to the conventional fuel baseline of 89.0 gCO_2eq/MJ. 95% of the values lie between 37.9 – 44.5 gCO_2e/MJ, while the median is equal to the mean and the skewness is 0.087. Also, the standard deviation is 1.74 gCO_2eq/MJ, and the kurtosis is 2.44. It was discovered that 13.6% of the emissions in this life cycle are from the wood residue collection, 30.1% are from the transportation stage, while 56.7% arise from the production of jet fuel. Lastly, the mean value which is 54% lower than the CORSIA value of 89.0 gCO_2e/MJ.

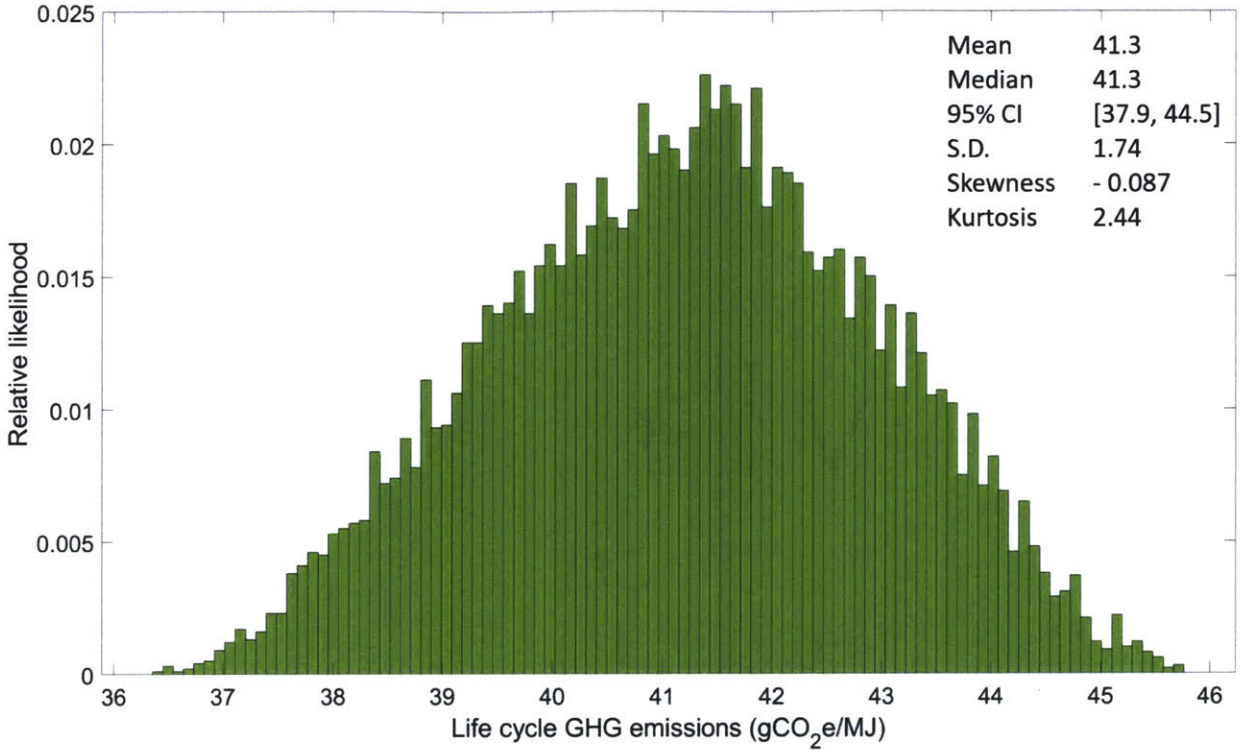

Figure 3-7: Monte Carlo simulation results for the micro FT fuel from forest residue LCA.

3.1.7 Fischer-Tropsch jet Fuel from Municipal Solid Waste

The stochastic LCA for the FT jet fuel from MSW pathway yielded a mean value of 36.3 gCO_2e/MJ for the total life cycle emissions. This represents a 60% reduction from the conventional jet fuel baseline emissions value of 89.0 gCO_2e/MJ [22]. 95% of the stochastic LCA results lie within 23.6 - 48.7 gCO_2e/MJ and the median with the mean. This indicates that our results are not particularly outlier-prone. The standard deviation takes on a large value of 6.50 gCO_2eq/MJ, while the skewness is - 0.055 and the kurtosis is 2.83. The CO_2e emissions absent the credits were also calculated, and the mean value was 79.5 gCO_2e/MJ. The percentage responsibility of each stage is as follows: transportation: 7.9%, jet fuel production: 51.7%, combustion: 40.4%. Finally, it should be noted that the mean emissions value of the overall LCA, 36.3 gCO_2e/MJ is 9.3% lower than the CORSIA determined life cycle value of 40.0 gCO_2e/MJ [22].

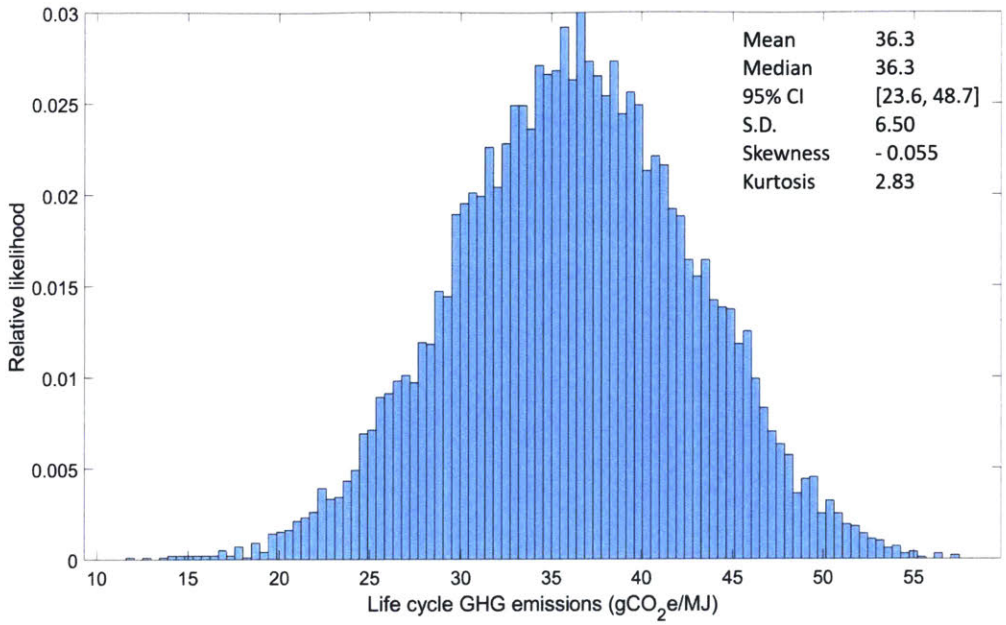

Figure 3-8: Monte Carlo simulation results for the FT fuel from MSW LCA.

3.2 Sensitivity Analysis

A sensitivity analysis of the life cycle CO_2e emissions was carried out for all the pathways included in this study. This was achieved by setting the parameter to a low value and then a high value while keeping the other stochastic parameters unaltered. The 2.5 percentile was chosen for the low value while the 97.5 percentile was chosen for the high value. Tornado charts were generated showing the average value of total emissions resulting from these changes to the parameters. The parameters were arranged in order of how sensitive the LCA results were to them taking on extreme values. It should be noted that crop yield, the quantity of the crop harvested per unit area of farmland, is inversely related to the life cycle emissions. It therefore resulted in lower emissions when taking on its 97.5 percentile (high) value and resulted in higher emissions when taking on its 2.5 percentile (low) value. Lastly, note that the feedstock-to-fuel ratio is the inverse of the fuel yield.

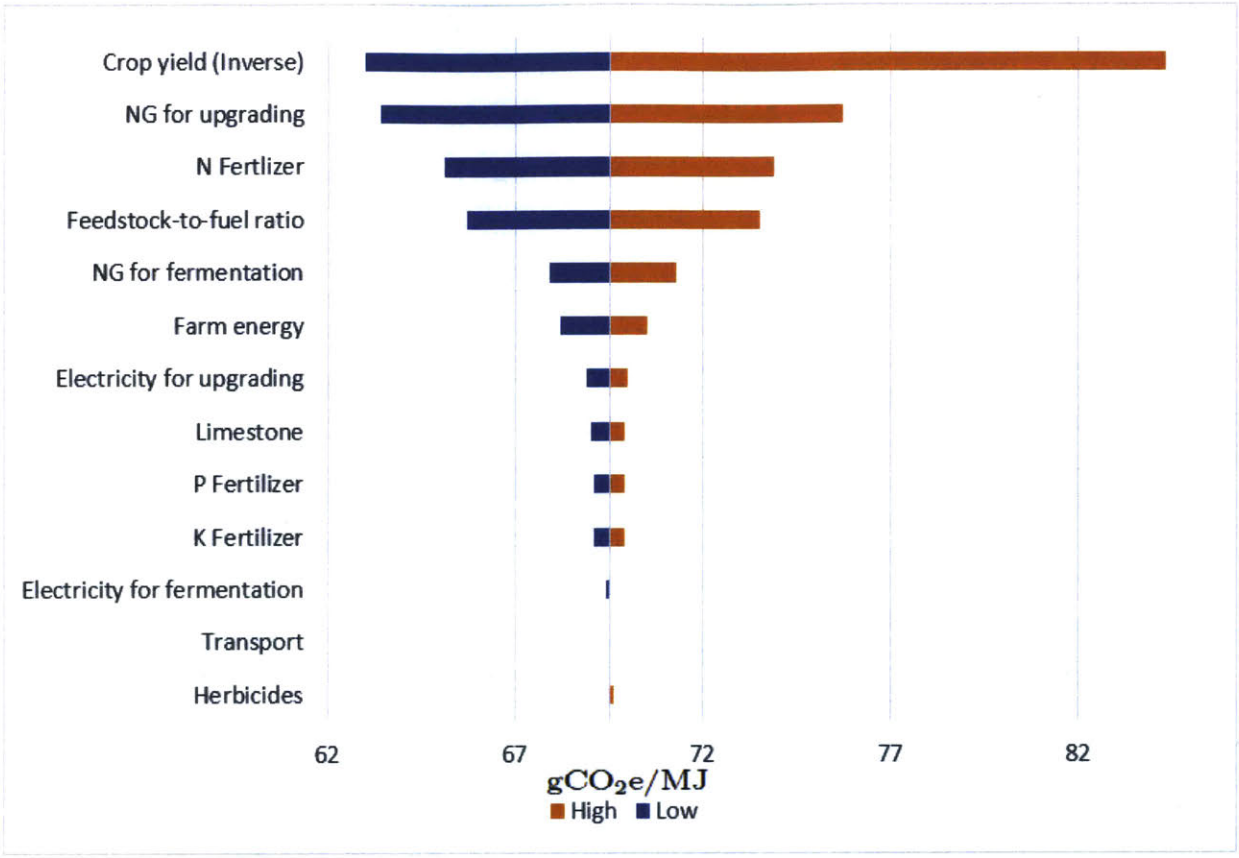

Figure 3-9: Life cycle CO_2e emissions sensitivity analysis for the corn ATJ pathway.

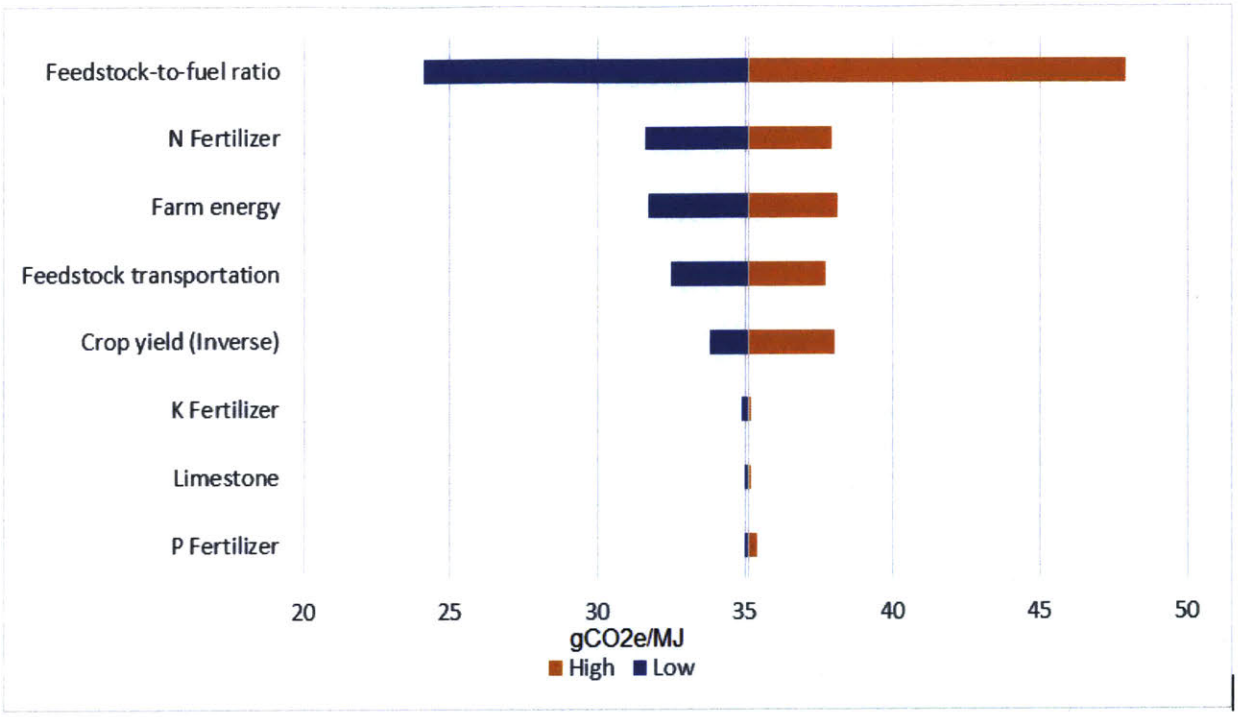

Figure 3-10: Life cycle CO_2e emissions sensitivity analysis for the sugarcane SIP pathway.

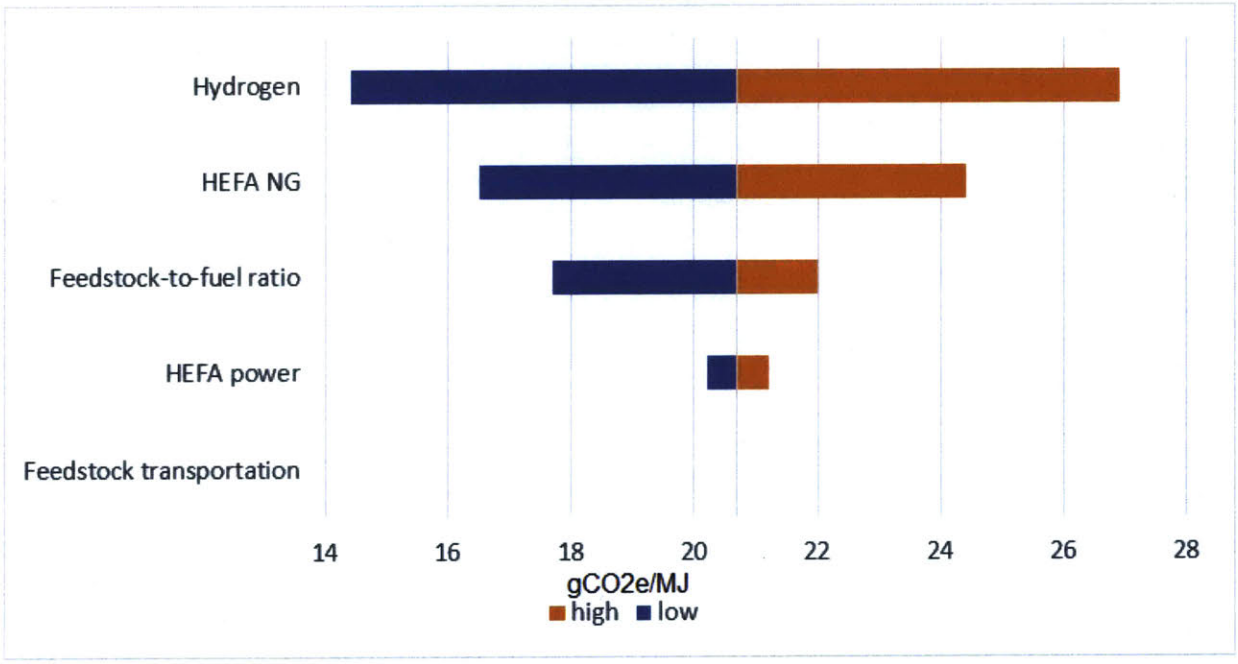

Figure 3-11: Life cycle CO_2e emissions sensitivity analysis for the HEFA PFAD pathway (System boundary I).

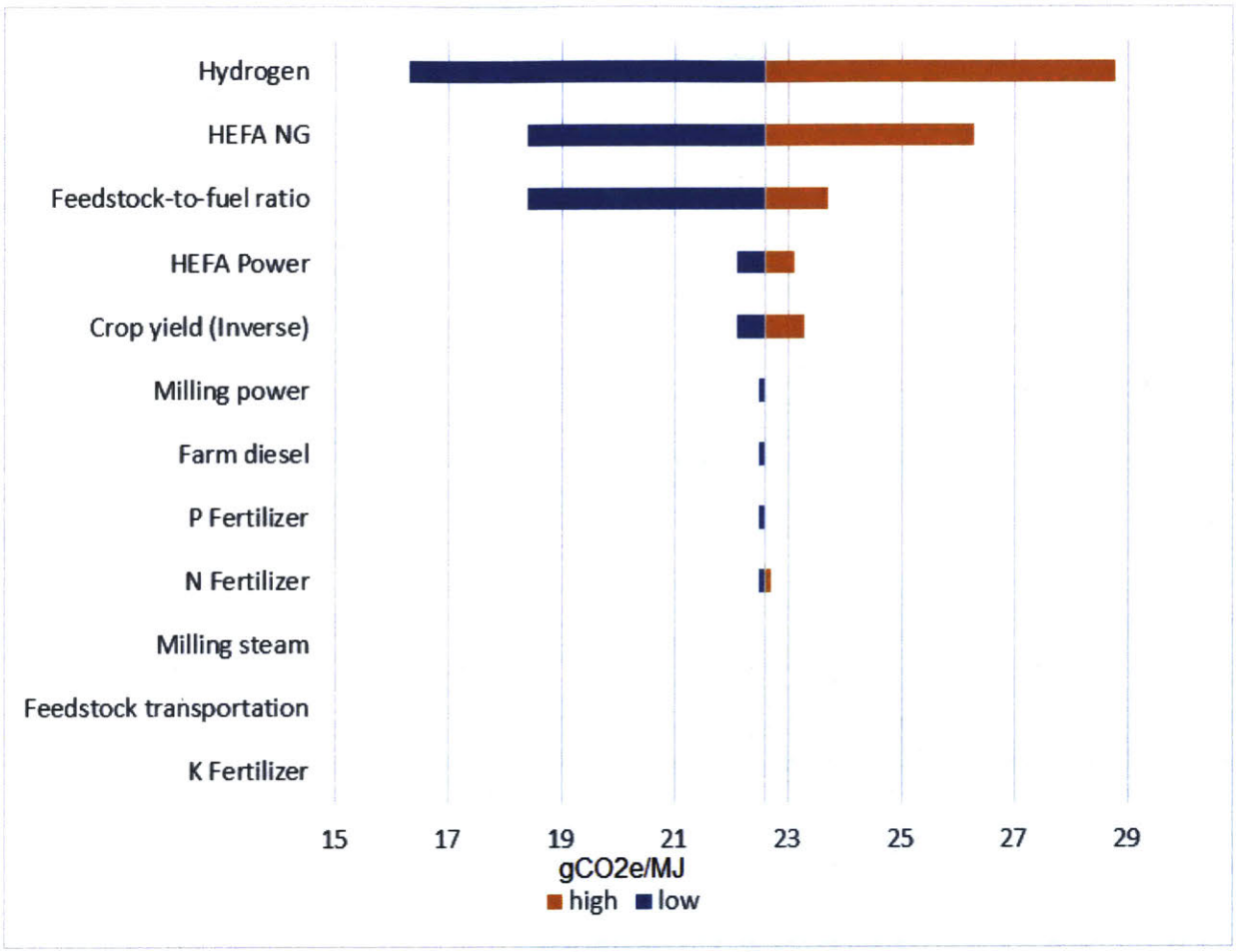

Figure 3-12: Life cycle CO_2e emissions sensitivity analysis for the HEFA PFAD pathway (System boundary II).

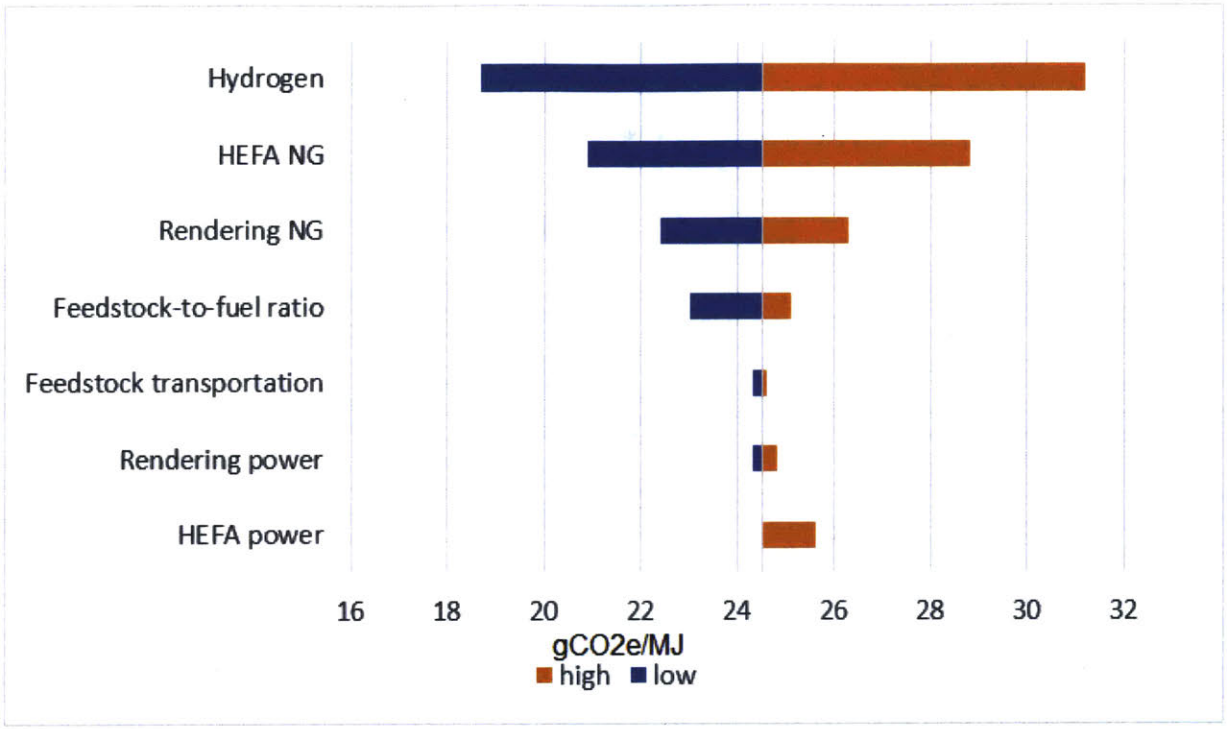

Figure 3-13: Life cycle CO_2e emissions sensitivity analysis for the HEFA FOG (Yellow grease) pathway.

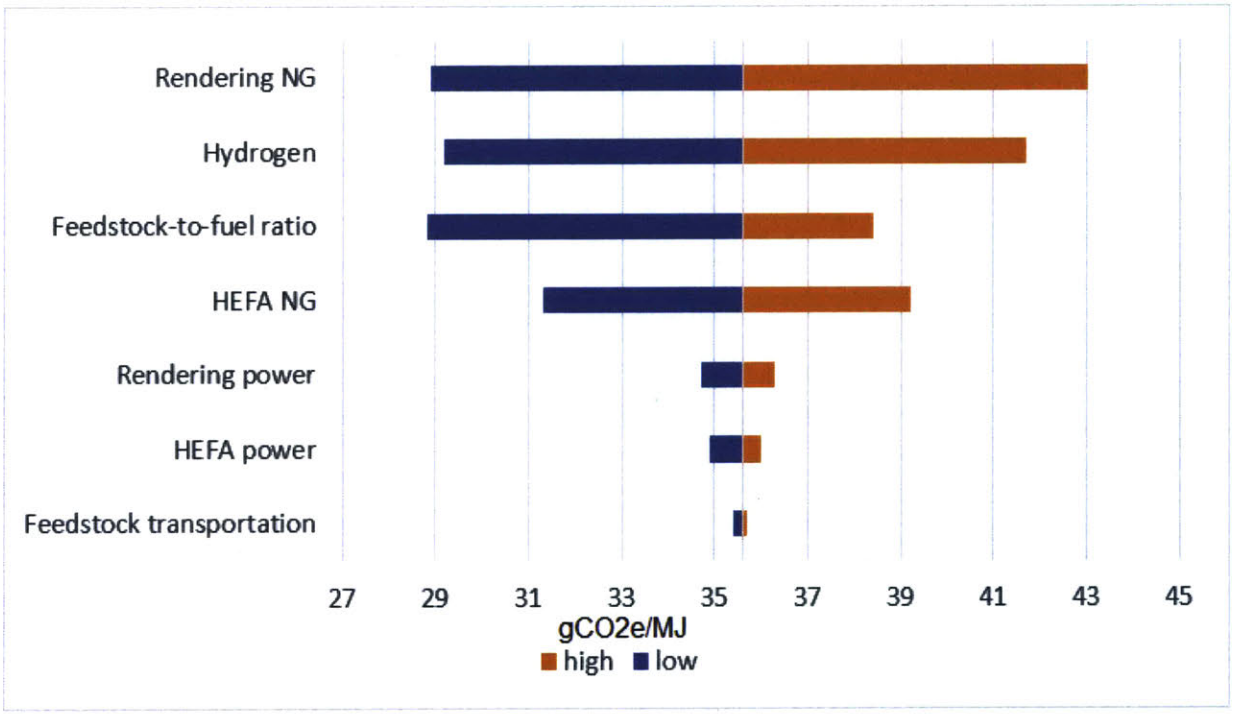

Figure 3-14: Life cycle CO_2e emissions sensitivity analysis for the HEFA FOG (Tallow) pathway.

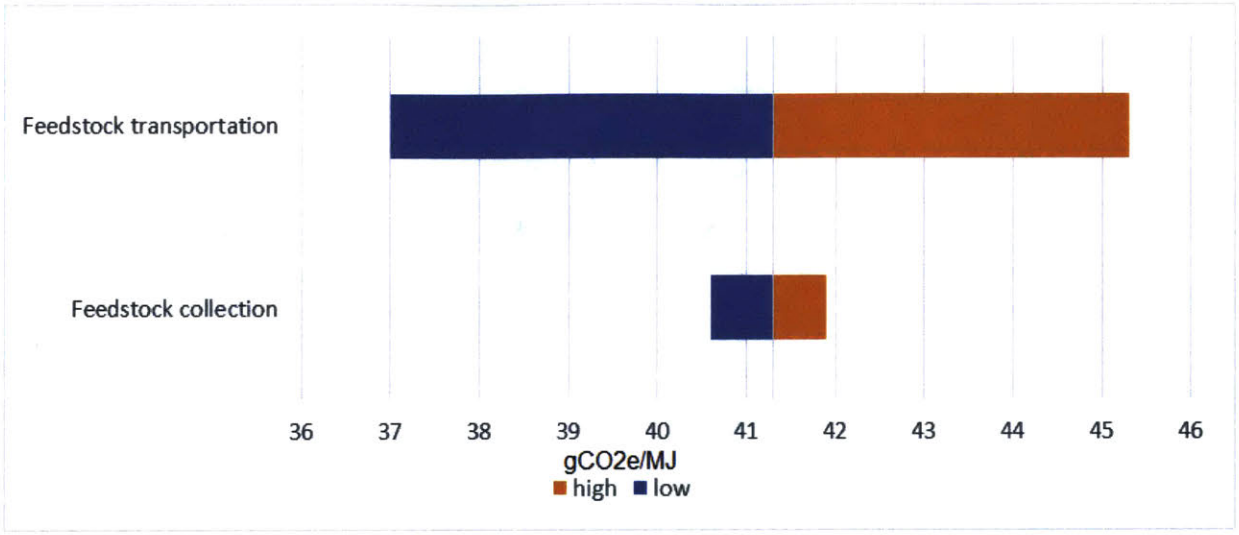

Figure 3-15: Life cycle CO_2e emissions sensitivity analysis for the micro FT jet fuel from forest residue pathway.

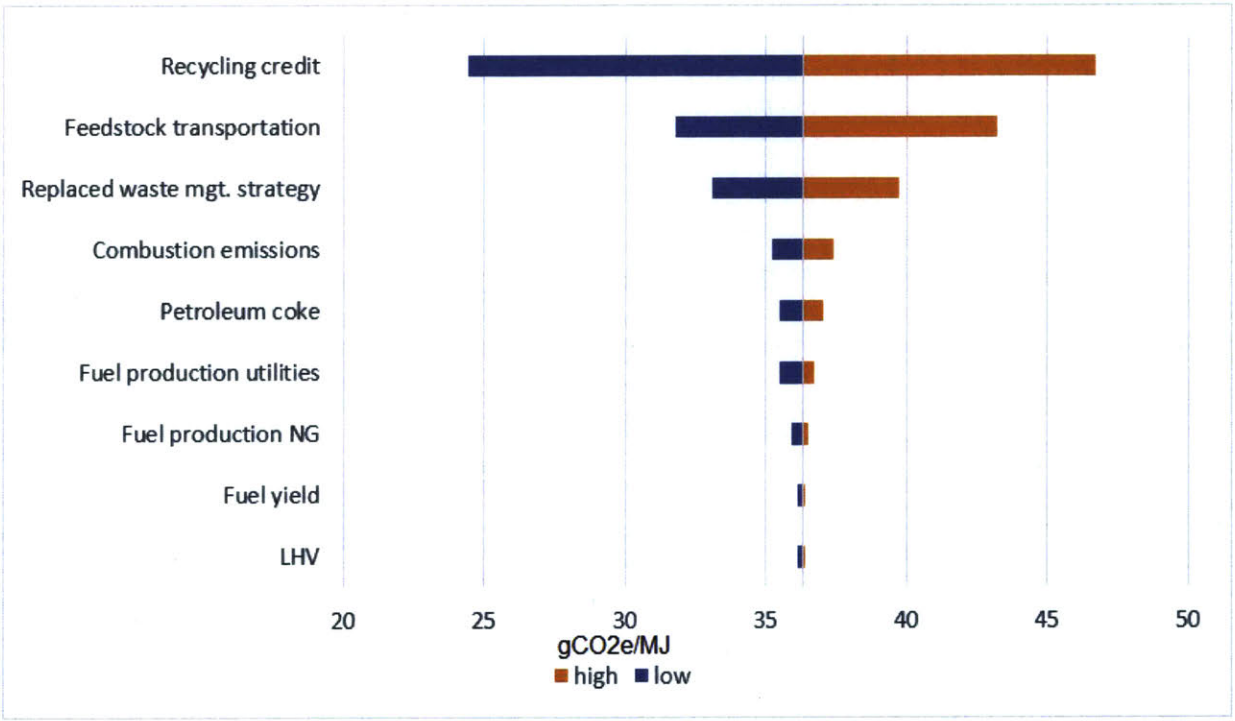

Figure 3-16: Life cycle CO_2e emissions sensitivity analysis for the FT jet fuel from MSW pathway.

3.3 Comparison of Stochastic LCA Results

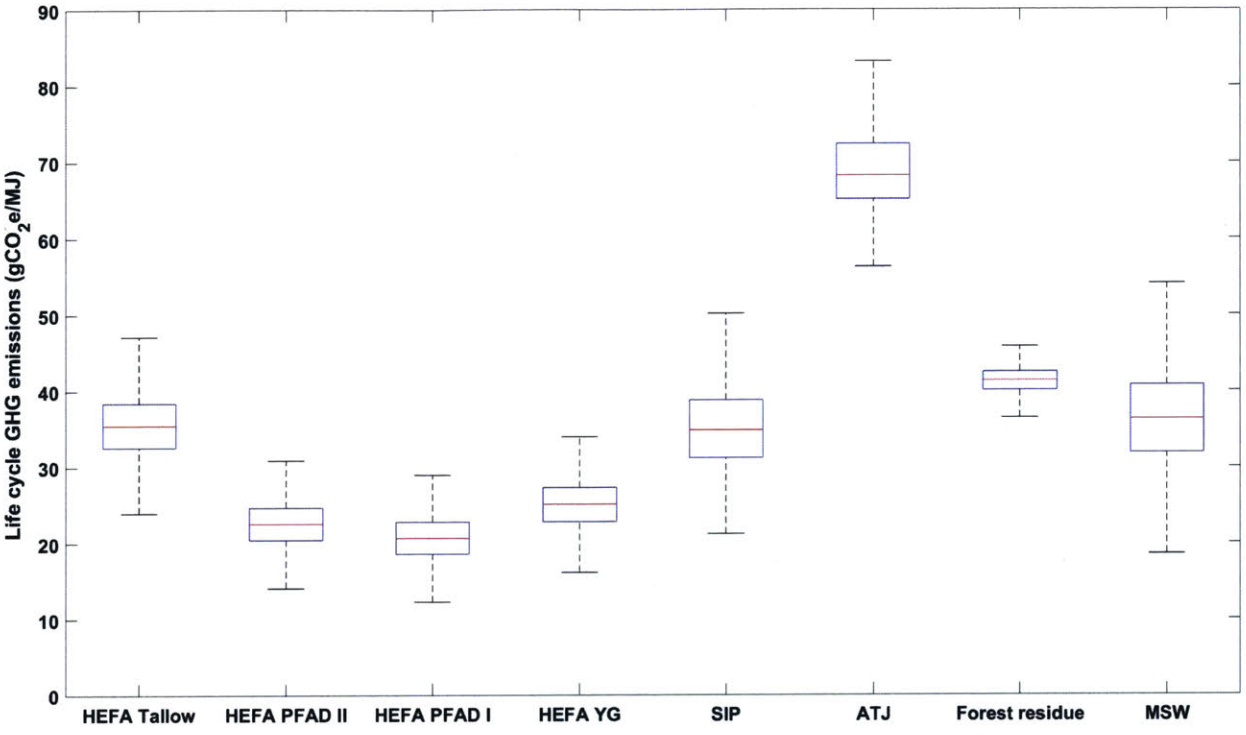

Figure 3-17: Comparison of stochastic LCA results for all pathways.

Figure 3-17 displays the results of the stochastic LCA for the renewable fuel pathways considered in this study. The red lines indicate the median value, while the boxes cover the interquartile range; with bottom and top at the 25^{th} and 75^{th} percentiles respectively. The black dotted lines extend to 1.5 times the interquartile distance away from the top and bottom of the respective boxes. It can be seen that the HEFA pathways take on relatively low values, while the corn ATJ has the highest median value. The interquartile range of the sugarcane SIP pathway is comparable to that of corn ATJ, while that of the forest residue pathway is small relative to others. This indicates that there is relatively low uncertainty in the forest residue pathway. It is also evident from the plot that the MSW pathway has a median comparable to that of HEFA FOG (Tallow) and Sugarcane SIP pathways, but has the widest interquartile range of all the pathways. A composite plot of the stochastic LCA histograms is found in Appendix E, and a comparison of mean stochastic LCA values with

the CORSIA determined values is found in Appendix C.

3.4 Stochastic Abatement Cost Assessment Results

3.4.1 Corn Alcohol-to-Jet (ATJ)

A paired Monte Carlo simulation was carried out for the stochastic LCA and stochastic TEA models, as the two models have some common parameters. The results of this simulation were used to calculate the greenhouse gas abatement cost based on conventional jet fuel price of \$0.50 per liter [44] and emissions of 89.0 gCO_2eq/MJ. This yielded an average value of \$1063.0/metric ton of CO_2e abated. 95% of the values lie between \$408.0 and \$2735.1, and the median was found to be \$917.5. The standard deviation is \$592.2, while the skewness is 2.580 and the kurtosis is 12.45.

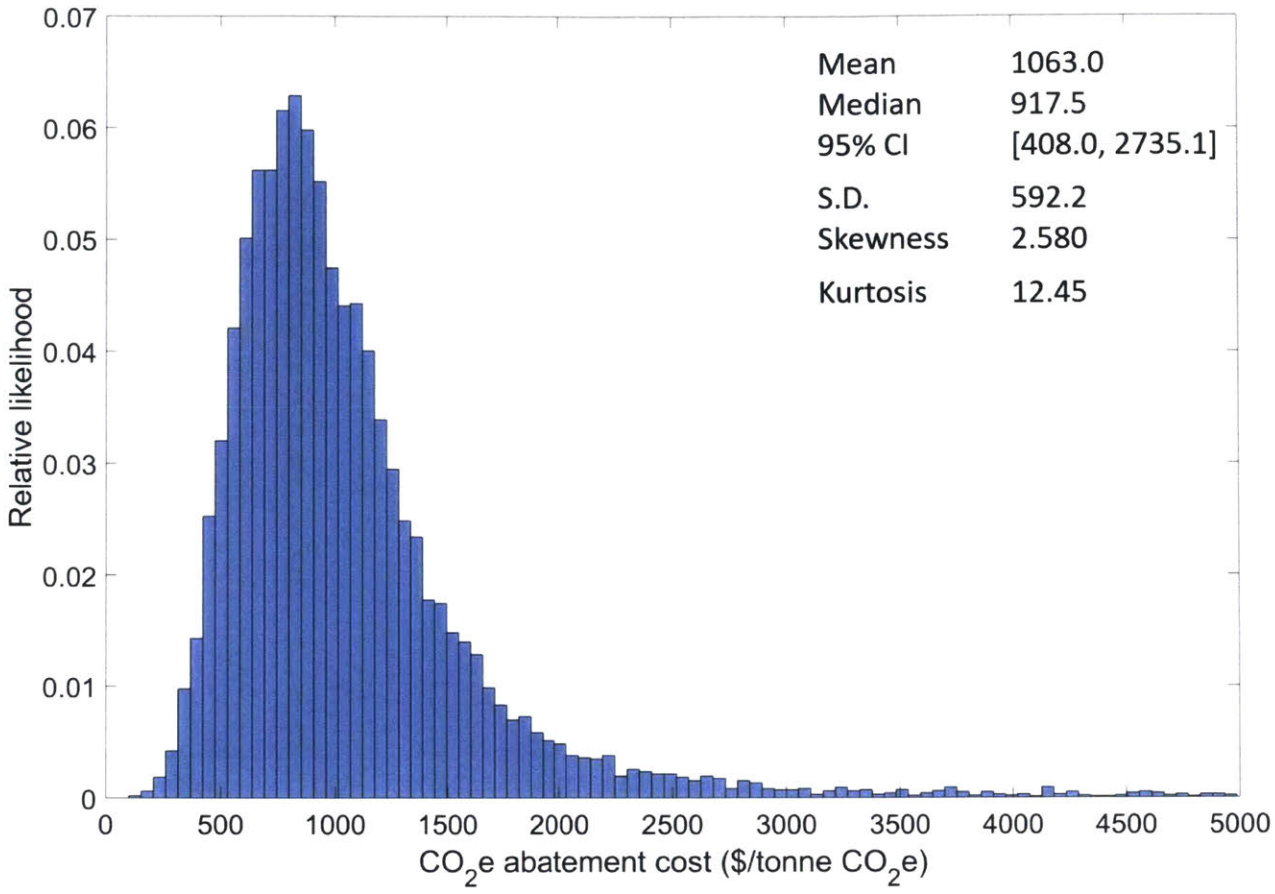

Figure 3-18: Monte Carlo simulation results for the corn ATJ CO_2e abatement cost.

3.4.2 Sugarcane SIP

The greenhouse gas abatement cost estimates were calculated based on conventional jet fuel price of \$0.50 per liter and emissions of 89.0 gCO_2e/MJ. This produced an average value of \$298.9/metric ton of CO_2eq. 95% of the values lie between \$87.6 and \$596.3 and the 50th percentile was found to be \$284.8. The standard deviation from the mean was found to be \$133.2, while the skewness is 0.654 and the kurtosis is 3.38. The histogram below captures all these statistical properties.

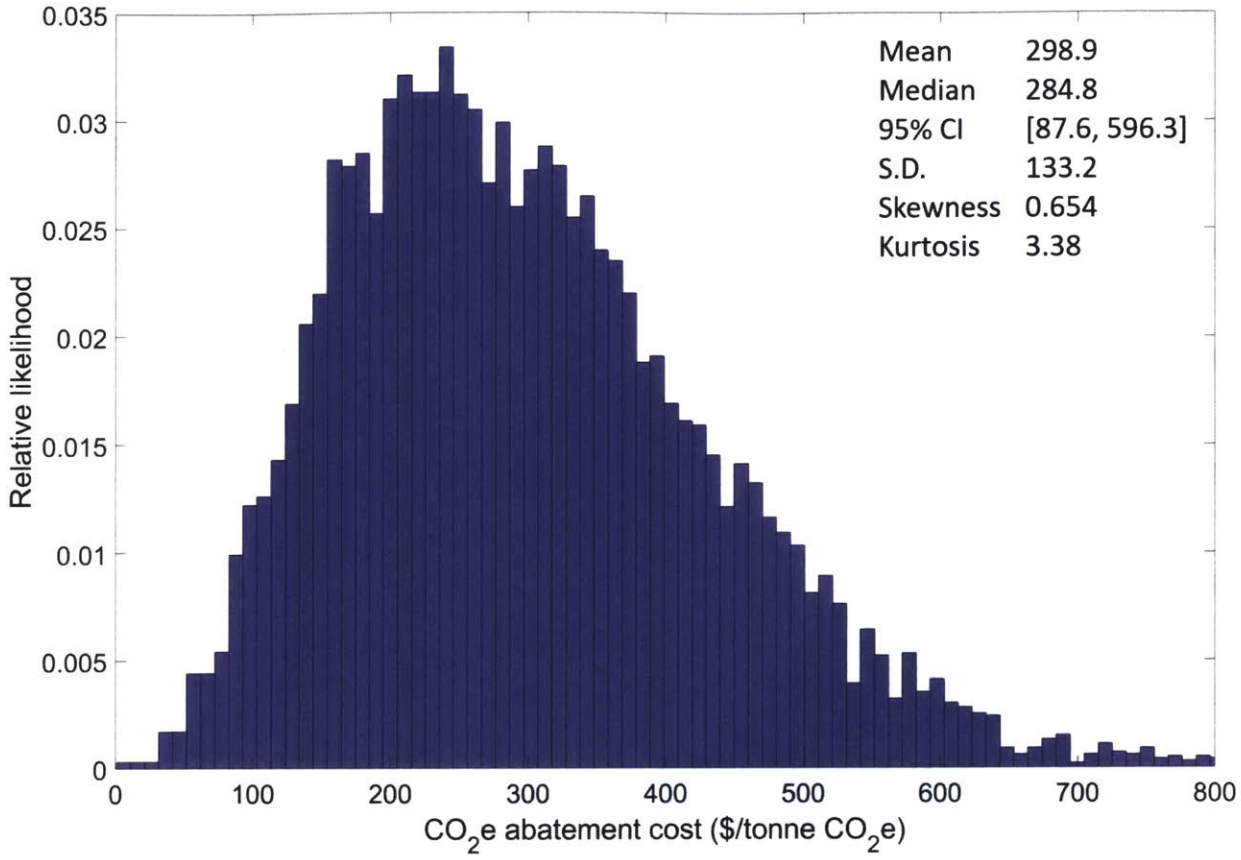

Figure 3-19: Monte Carlo simulation results for the sugarcane SIP CO_2e abatement cost.

3.4.3 HEFA PFAD

The LCA and TEA Monte Carlo models for the HEFA PFAD pathway were used to calculate the greenhouse gas abatement cost based on conventional jet fuel price of \$0.50 per liter and emissions of 89.0 gCO_2e/MJ. This average value obtained was \$97.5/metric ton of CO_2e. 95% of the values lie between \$25 and \$179 and the 50th percentile is \$96.2. The standard deviation was found to be \$40.0, while the skewness is 0.285 and the kurtosis is 3.05.

Due to the higher value of emissions realized in system boundary II, the abatement costs took on higher values on average in this case than the previous one. And the standard deviation, skewness, and kurtosis all differed from their values in system boundary I by less than 4%.

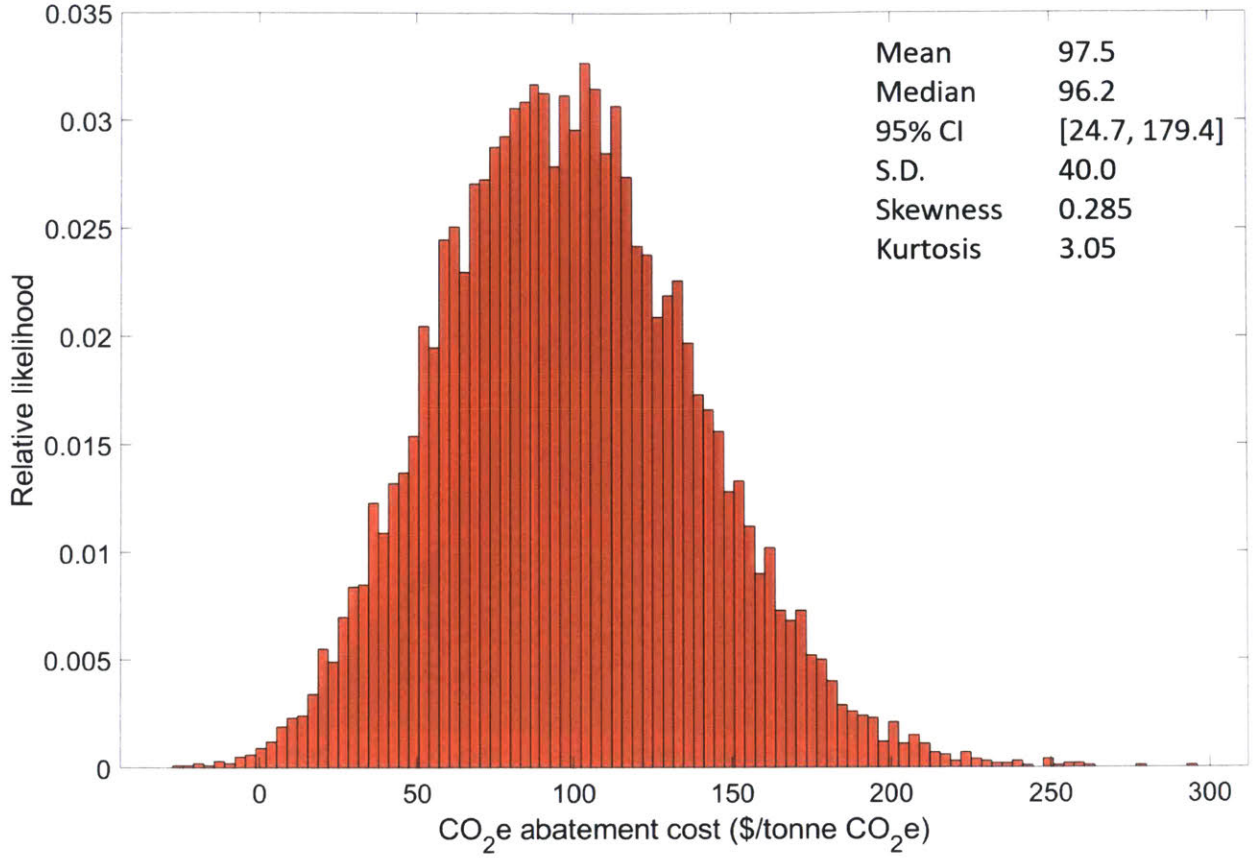

Figure 3-20: Monte Carlo simulation results for the HEFA PFAD (System boundary I) CO_2e abatement cost.

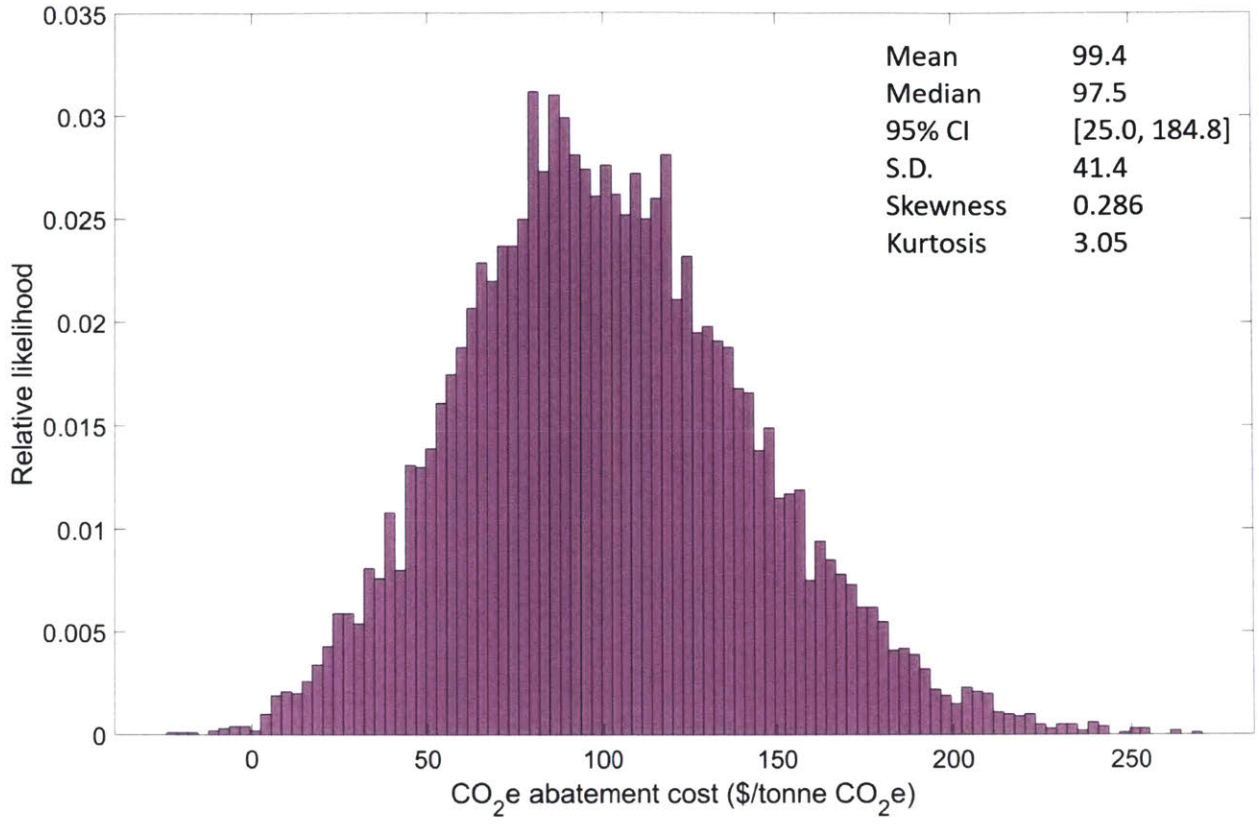

Figure 3-21: Monte Carlo simulation results for the HEFA PFAD (System boundary II) CO_2e abatement cost.

3.4.4 HEFA FOG (Yellow grease)

The LCA and TEA Monte Carlo results for the HEFA from yellow grease were used to calculate the greenhouse gas abatement cost based on conventional jet fuel price of $0.50 per liter and emissions of 89.0 gCO_2eq/MJ. This yielded an average value of $22.3/metric ton of CO_2e. 95% of the values lie between $- 62.8 and $101.1 and the 50th percentile was found to be $25.3. The standard deviation is $46.2, while the skewness was found to be - 0.076, and te kurtosis is 2.13. Finally, the abatement cost takes on many negative values. This is because based on the stochastic TEA model, HEFA FOG fuel sometimes has minimum selling price (MSP) values that are lower than $0.50 - the selling price of conventional jet fuel assumed for this study. Refer to Appendix D for the MSP values.

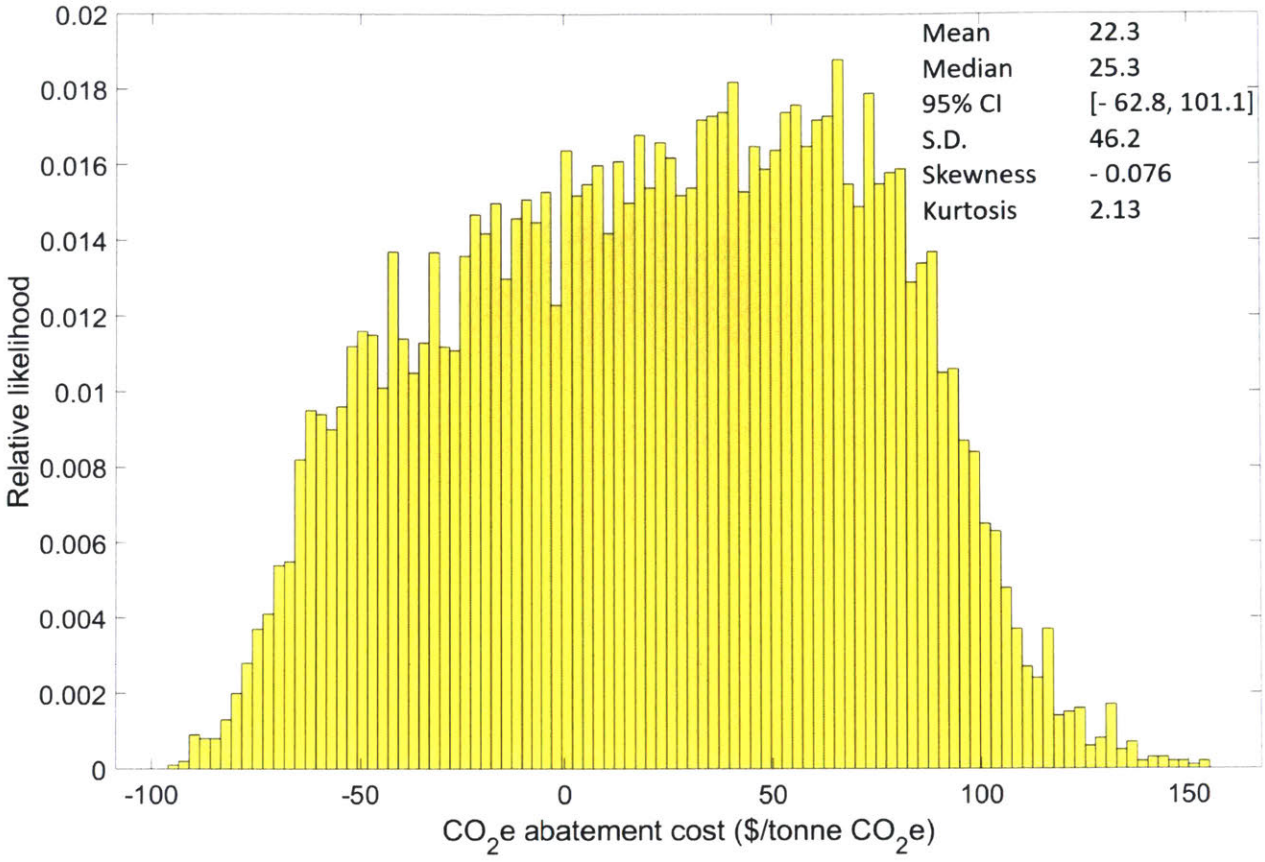

Figure 3-22: Monte Carlo simulation results for the HEFA FOG (Yellow grease) CO_2e abatement cost.

3.4.5 HEFA FOG (Tallow)

The LCA and TEA Monte Carlo results for the HEFA from beef tallow pathway were used to calculate the greenhouse gas abatement cost based on conventional jet fuel price of \$0.50 per liter and emissions of 89.0 gCO_2eq/MJ. This yielded an average value of \$25.9/metric ton of CO_2eq. 95% of the values lie between \$-74.6 and \$122.0 and the median was found to be \$29.6. Finally, The standard deviation from the mean is \$55.0, the skewness is - 0.069, and the kurtosis is 2.18.

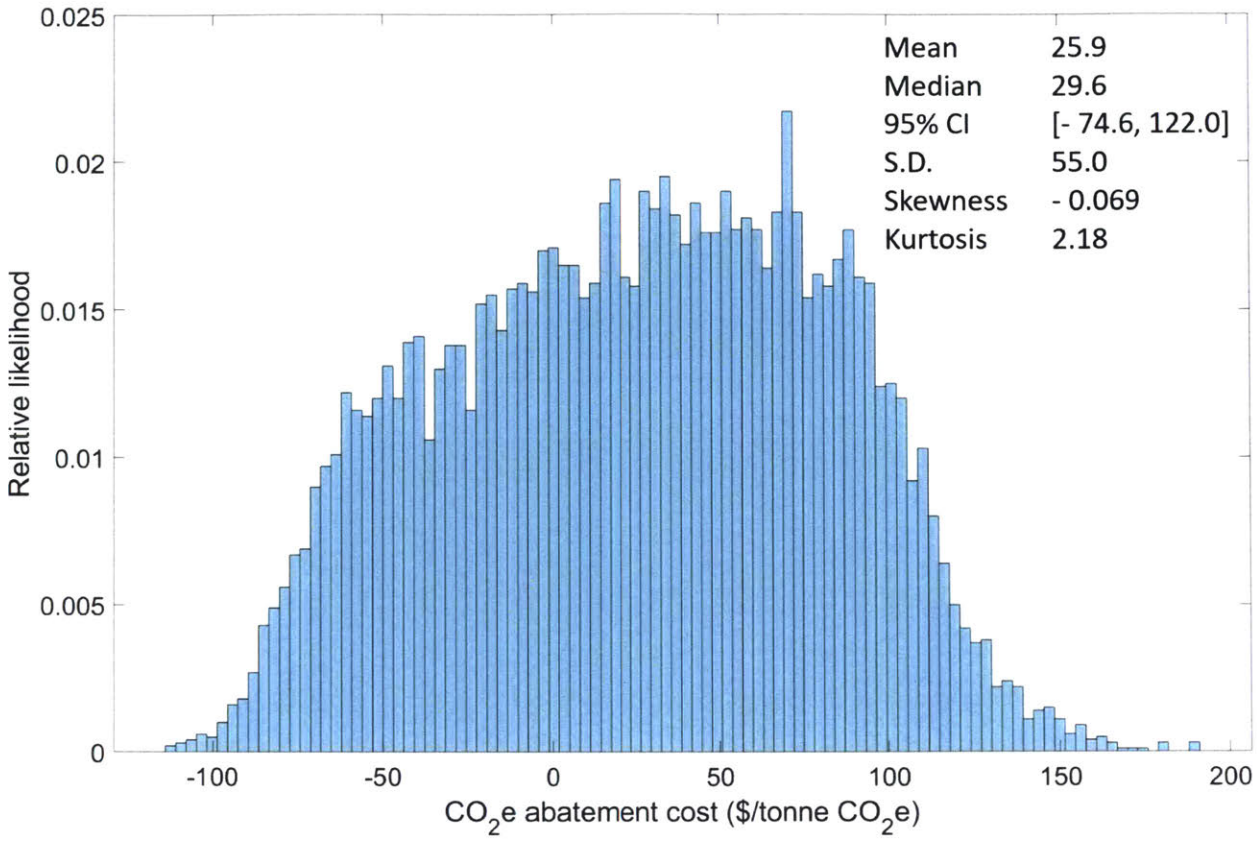

Figure 3-23: Monte Carlo simulation results for the HEFA FOG (Tallow) CO_2e abatement cost.

3.4.6 Micro Fischer-Tropsch Jet Fuel from Forest Residue

The LCA and TEA Monte Carlo results for the HEFA from beef tallow pathway were used to calculate the greenhouse gas abatement cost based on conventional jet fuel price of \$0.50 per liter and emissions of 89.0 gCO_2eq/MJ. This yielded an average value of \$532.3/metric ton of CO_2e. 95% of the values lie between \$394.6 and \$689.0, and the 50th percentile was found to be \$528.7. The standard deviation is \$76.55, while the skewness is 0.235, and the kurtosis is 2.76.

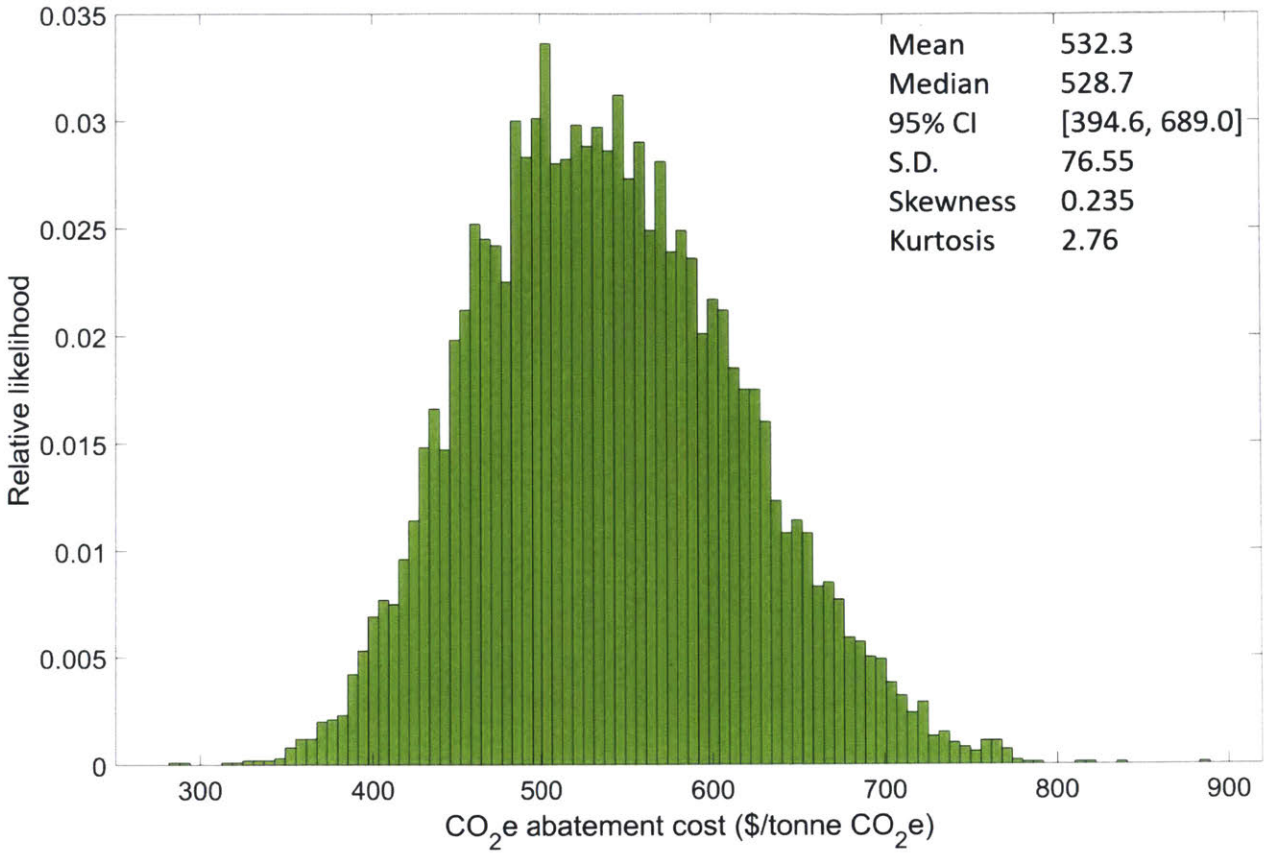

Figure 3-24: Monte Carlo simulation results for the micro FT fuel from forest residue CO_2e abatement cost.

3.4.7 Fischer-Tropsch Jet Fuel from Municipal Solid Waste

The LCA and TEA Monte Carlo results for the FT jet fuel from MSW pathway were used to calculate the greenhouse gas abatement cost based on conventional jet fuel price of \$0.50 per liter and emissions of 89.0 gCO_2eq/MJ. This yielded an average value of \$210.8/metric ton of CO_2e. 95% of the values lie between \$66.6 and \$377.7, and the 50th percentile is \$207. The standard deviation was found to be \$79.4, while the skewness is 0.690, and the kurtosis is 3.71.

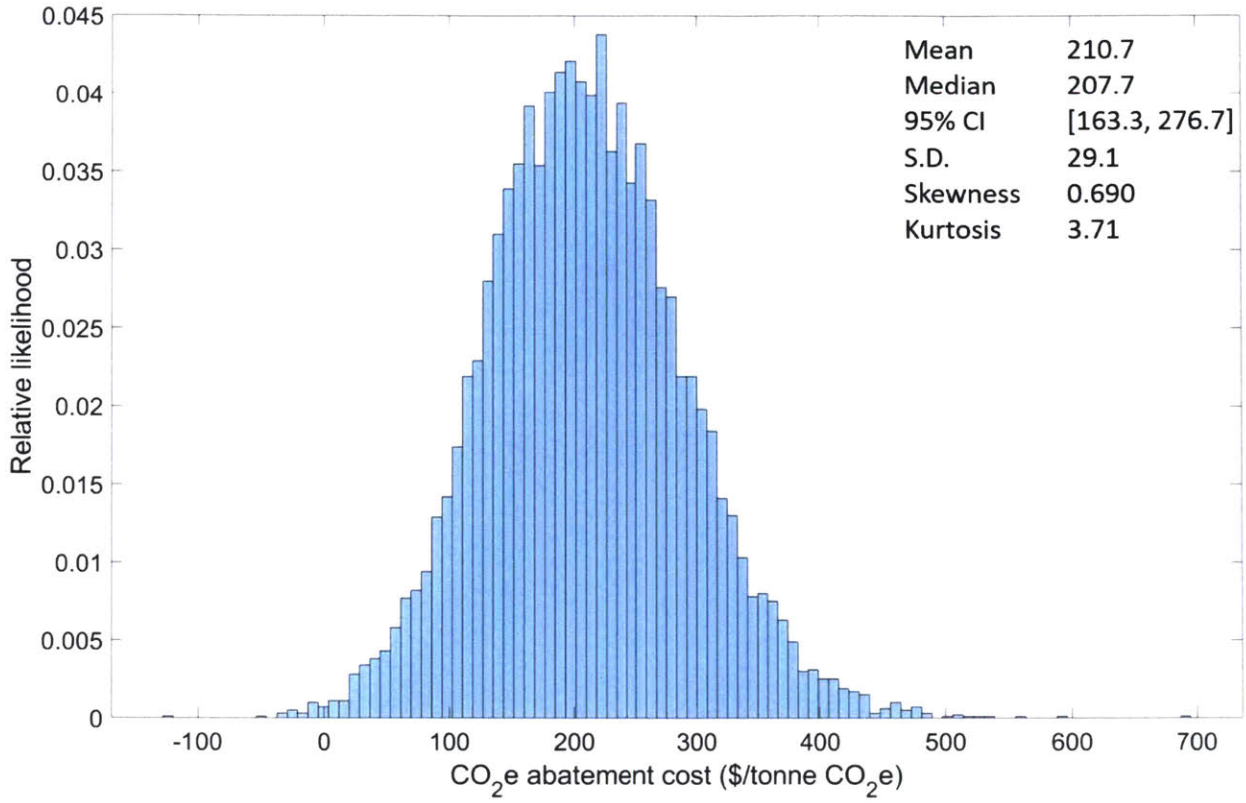

Figure 3-25: Monte Carlo simulation results for the FT fuel from MSW CO_2e abatement cost.

3.5 Abatement Cost Comparisons

3.5.1 Comparison of Renewable Fuel Pathways

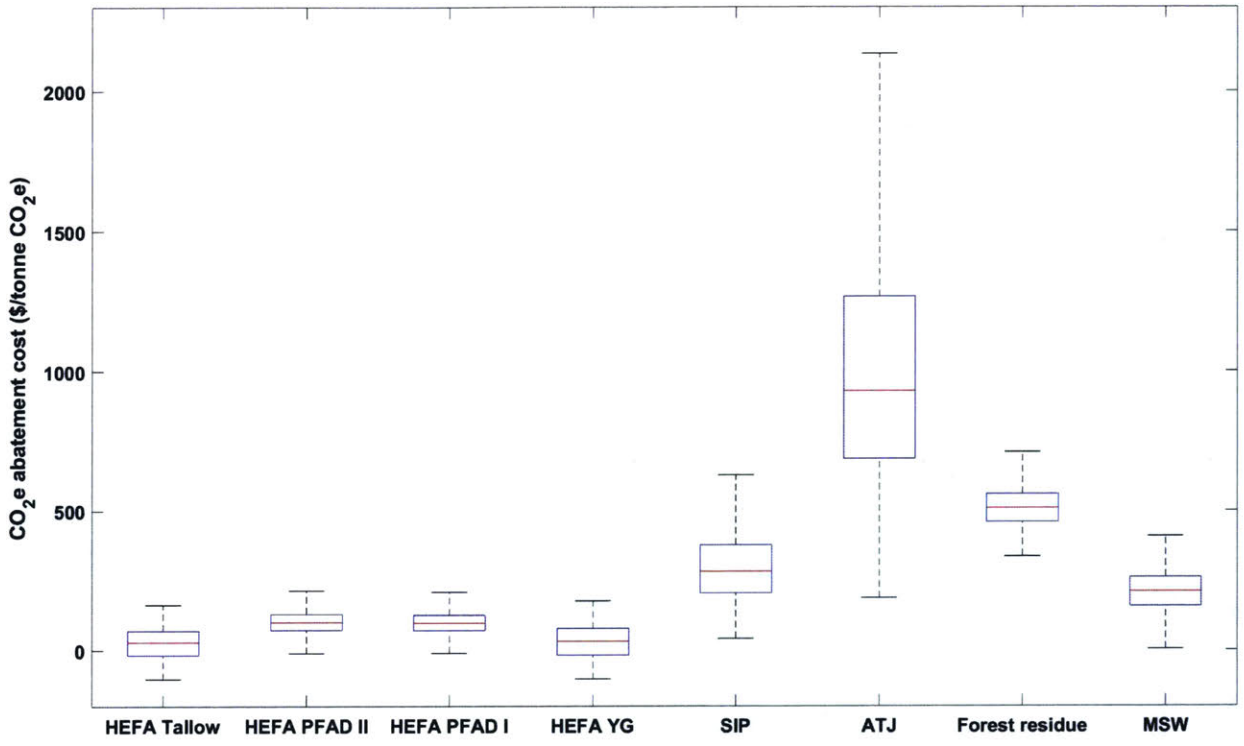

Figure 3-26: Comparison of stochastic abatement cost results for all pathways.

Figure 3-34 displays the results of the stochastic abatement cost assessment for the renewable fuel pathways considered in this study. The red lines indicate the median value, while the boxes cover the interquartile range; with bottom and top at the 25th and 75th percentiles respectively. The black dotted lines extend to 1.5 times the interquartile distance away from the top and bottom of the respective boxes. It can be noticed that the HEFA pathways give the lowest abatement cost values, which is due to the relatively low LCA emissions and MSP values. The corn ATJ pathway takes on the largest values and has the widest interquartile range of all the pathways. These properties indicate that the corn ATJ is both the most uncertain and the most expensive from a climate change mitigation standpoint. Also, the sugarcane SIP pathway has the second largest interquartile range, and the forest residue

pathway has the second highest median and quartile values. Lastly, the MSW pathway is of comparable interquartile range to the forest residue pathway but takes on values closer to those of the HEFA pathways.

3.5.2 Comparison with other GHG Abatement Options

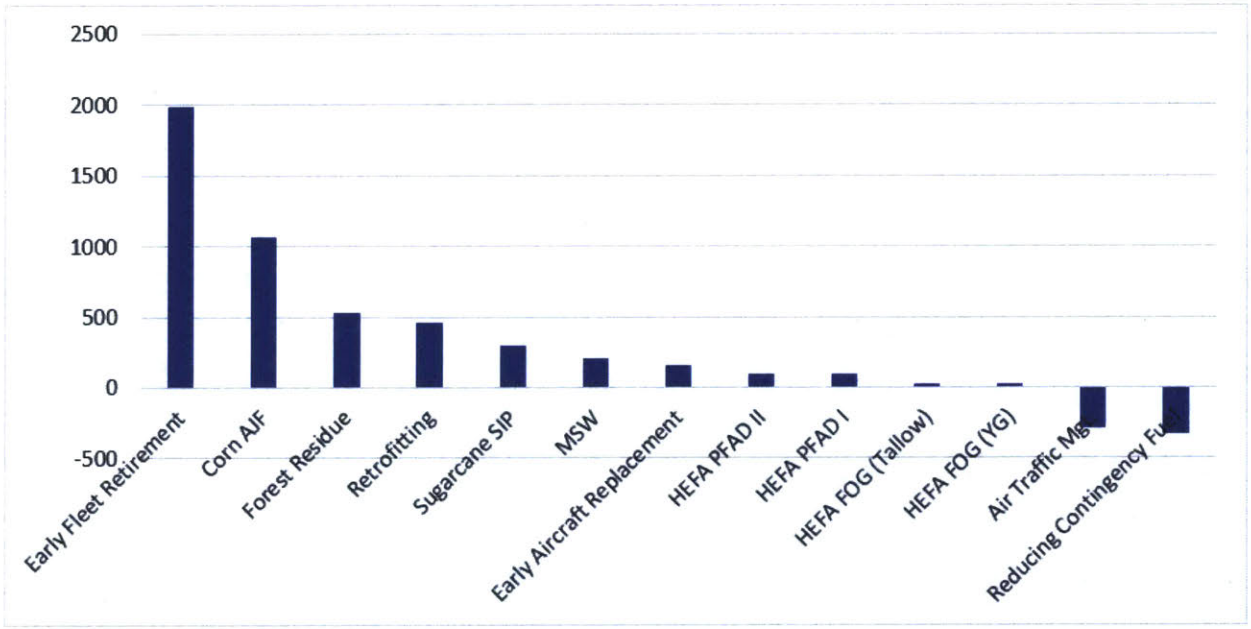

Figure 3-27: Comparison of abatement costs ($/tonne CO_2e) of renewable fuel pathways and other GHG abatement options.

Figure 3-35 shows the average CO_2e abatement cost values for the pathways in this study alongside the abatement costs of some other options. Early fleet retirement has an abatement cost of around $1991/tonne CO_2e [45] and is more costly than all the renewable drop-in fuels considered. Retrofitting engines with energy efficient technologies is another GHG mitigation option, with abatement costs in the region of $456/tonne CO_2e [45]. Replacement of aircraft of 25 years or older with intermediate generation aircraft in 2020 is expected to have an abatement cost of around $160/tonne CO_2e [47]. This value is lower than the mean abatement costs of all the non-HEFA fuels considered in this study. Improvements in air traffic management and the reduction of contingency fuels by 300 kg have negative abatement

cost values associated with them [47]. There are other abatement options outside of these outlined here, such as increasing of load factor, electric taxiing, and surface congestion management [46]. It is important to recognize that the stochastic techno-economic analysis (TEA) used to generate the abatement costs for the renewable fuels was carried out under a no policy assumption [42]. This means that there is a possibility of these fuels having a lower MSP and hence lower abatement costs if the appropriate policies are introduced. The following chapter will address this subject.

Chapter 4

Policy

4.1 Policy Measures for Renewable Fuels

Biofuels are among the few feasible options for reducing the climate impact of aviation in the near-to-medium term [47]. Notwithstanding, there are many factors such as high production costs and limited resource availability which make the adoption of these biofuels quite challenging [49]. Production costs of renewable fuels have been estimated to lie between $2 to $10 per gallon [49] and feedstock availability for some pathways such as HEFA has proven to be an obstacle to scaling the AJF production to the required level [47]. Lastly, these challenges lead to high prices of renewable jet fuels as compared to conventional, kerosene-based jet fuel. And considering that jet fuel constitutes about 27% of airline operational expenses [48], it is unlikely that renewable fuels would be adopted by airlines unless their production is subsidized through policy instruments. In line with this, there have been a number of policy measures taken by different governments and bodies which have aimed to promote the use of biofuels [49]. For example, in June 2011, the private-public program European Advanced Biofuels Flightpath (EABF) which set a target of having 2 million tonnes of biofuels used in the EU by the year 2020 [50], later deferred to 2030. The project aims to achieve this goal through accelerating biofuel technology research and innovation

and establishing appropriate financing structures to facilitate completion of biofuel projects, amongst other actions [51].

In the United States, several government bodies such as the Department of Agriculture (DOA), Internal Revenue Service (IRS), Department of Energy (DOE), and the Environmental Protection Agency (EPA) have introduced programs to achieve increased biofuel production and usage [51]. These programs collectively involve: Tax credits for biofuel producers, financial assistance for establishment and expansion of plants, research and development funding, reduction of import duties for certain biofuels, and the provision of incentives to manufacturers [51].

4.2 Application of Stochastic LCA and Abatement Cost Assessment to Aviation Policy

To adequately determine the carbon footprint and hence, the GHG emissions reduction from using a renewable fuel, all emissions in the fuel production life cycle need to be properly accounted for [9]. With the knowledge of the level of GHG emissions reduction, an airline and regulatory bodies can ascertain how much carbon credits the airline should receive for using the drop-in fuel for its aircraft. The stochastic LCA quantifies uncertainty in life cycle emissions and thus gives policy makers an understanding of the likelihoods of different emissions values and the hence the risk associated with basing decisions on a particular emissions value or value range. The GHG abatement cost of a drop-in fuel is the dollar cost to consumers of the fuel, of reducing CO_2e emissions by 1 tonne. The stochastic abatement cost assessment gives probabilistic estimates of the abatement costs of the fuel. This quantification of uncertainty is highly useful from an investment standpoint as it provides information on the mathematical risk of investing in the fuel, which in turn informs business decisions and strategies. Also, the assessment provides information on the relative likelihood of abatement cost values for the biofuels compared to each other. This is relevant from an environmental

policy standpoint as it informs decision-making regarding the allocation resources to the promotion of each fuel. And crucially, the stochastic abatement cost assessment allows us to have a detailed economic comparison of these renewable fuels to other GHG mitigation options and technologies.

Chapter 5

Conclusions

This thesis quantifies the inherent technical uncertainty in the life cycle GHG emissions and associated abatement costs of six renewable drop-in fuel pathways. This was intended to improve upon existing studies which produced deterministic estimates for these quantities. The methodology included first understanding and modeling the fuel production pathway and identifying parameters which appear to be stochastic. The subsequent steps were the collection of data for these parameters and defining the probability density functions (PDF) for them. A Monte Carlo simulation was then carried out with randomly generated inputs from the aforementioned distributions, yielding a histogram of the possible LCA emissions values. To compute the stochastic abatement cost values, the stochastic LCA was paired with the stochastic TEA and their outputs were compared with the conventional jet fuel baseline emissions value of 89.0 gCO_2e/MJ and baseline price per litre of \$0.50. It was observed that the corn ATJ pathway had the highest average value of life cycle CO_2e emissions, 69.5 gCO_2e/MJ. The lowest was from the HEFA PFAD pathway, 20.7 gCO_2e/MJ when PFAD is considered as a waste product (system boundary I), and 22.6 gCO_2e/MJ when it is considered a valuable resource (system boundary II). Overall, the LCA results in this study showed that there is considerable variance in life cycle emissions of renewable drop-in fuels.

A comprehensive sensitivity analysis was also carried out to better understand the influ-

ence of the various stochastic parameters on the total life cycle emissions. The stochastic abatement cost assessment results were also analyzed, and it was found that the average values for the corn ATJ pathway were about 50 times that of the HEFA FOG pathways. This indicates that the corn ATJ fuel would most likely require significant subsidization to be a feasible fuel option for airlines. The abatement costs were also compared to some other abatement strategies. The relevance of this study to aviation policy was also discussed as these detailed results could offer valuable insights to policy makers. The results provide a quantification of the relative likelihood of different outcomes, which in turn provides a better understanding of the potential costs, benefits, and risks associated with these fuels than a deterministic analysis does. The stochastic assessments of these pathways could be improved upon in the future through gathering of more data, as a larger amount of data would lead to a model that offers a more accurate mathematical representation of the phenomena under study. Also, future work could involve a similar investigation of other renewable drop-in fuel pathways.

Appendix A

Overview of Fuel Production Technologies

A.1 Advanced Fermentation (AF)

The production of isobutanol from corn grain is achieved through advanced fermentation (AF). The corn grain can be either dry milled or wet milled, in either case, the corn is broken down and mixed with water at a high temperature to produce a slurry [52]. This slurry is then put through liquefaction and saccharification which produces glucose, fructose, and xylose [43, 52]. After this, the glucose is then metabolized into isobutanol through the action of yeast. Ammonium sulfate ($(NH_4)_2SO_4$) or urea is also added, and the alcohol is further distilled after this process [52]. Finally, the isobutanol is upgraded to jet fuel [7, 43].

A.2 Hydroprocessed Esters & Fatty Acids (HEFA)

In the hydroprocessed esters and fatty acids (HEFA) process, the oil feedstock is fed into a hydrotreater with gaseous hydrogen. This deoxygenates the oil, which is then cooled by steam generation, and subsequently isomerized. It is then cooled and passed through separation units yielding paraffins, carbon dioxide, and excess hydrogen. The paraffins and

hydrogen are reused in the hydrotreater, and the liquid products streams are separated into LPG, naphtha, jet fuel, and diesel. [10, 43, 53].

A.3 Conventional Gasification and Fischer-Tropsch (FT) Synthesis

The municipal solid waste (MSW) feedstock initially goes through sorting and removal of non-combustibles and other inorganics [43]. It is subsequently partially oxidized at a high temperature and in a limited amount of air. This produces syngas which is then cooled, conditioned, and synthesized to produce fuels and paraffinic wax using a Fischer-Tropsch catalyst [25, 54]. These products are then refined into jet fuel, diesel, and naphtha - which is converted to gasoline [25]. The Fischer-Tropsch process produces large amounts of energy, which along with unconverted syngas, is used for feedstock drying and electricity generation [25, 34, 35].

A.4 Synthetic Iso-Paraffinic Kerosene (SIP)

The production of synthetic iso-paraffins is through the Fischer-Tropsch process. The first step is the use of a Fischer-Tropsch catalyst to synthesize a heavy hydrocarbon mixture which contains paraffins. Some of this is then converted to iso-paraffins through hydrocracking with a hydrocracking/isomerization catalyst. The iso-paraffins are then separated out from other paraffinic materials, and a portion of these paraffins is recycled [55].

A.5 Micro Fischer-Tropsch Synthesis

A Microreactor or microchannel reactor is a device in which chemical reactions take place in a confined space with lateral dimensions less than 1mm. Microreactors typically facilitate

chemical reactions in a continuous stream and are advantageous in that they are more energy efficient, have higher reaction yield, and have better process control [56]. They also promote fast reaction rates through minimization of heat and mass transport limitations [57, 58]. The potential of heat-exchange micro reactors to minimize Fischer-Tropsch synthesis heat transfer problems has been studied extensively [57].

Appendix B

Emissions Indices

Table B.1: Emissions indices for physical inputs. [11]

Parameter	CO_2e index	N_2O index	CH_4 index	Unit
N Fertilizer	3.887	0.026	0.011	g/g
P Fertilizer	1.338	0	0.003	g/g
K Fertilizer	0.566	0	0.001	g/g
Herbicides	18.678	0.002	0.039	g/g
Limestone	0.227	0	0	g/g
Diesel	86.778	0	0.164	g/MJ
LPG	75.802	0.008	0.176	g/MJ
Natural gas	60.121	0	0.586	g/MJ
Electricity	97.98	0.0022	0.3	g/MJ

Appendix C

Comparison of Stochastic LCA Results with CORSIA Values

Table C.1: Stochastic LCA values compared to CORSIA deterministic values (gCO_2e/MJ).

Pathway	CORSIA value	Stochastic LCA mean value	Percentage difference (%)
Corn ATJ	75.0	69.5	- 7.3
Sugarcane SIP	50.6	35.1	- 30.6
HEFA PFAD	20.7	20.7, 22.6	0, 9.2
HEFA FOG	22.5	24.5, 35.6	8.9, 58.2
Micro FT fuel from forest residue	89.0	41.3	- 53.6
FT fuel from MSW	40.0	36.3	- 9.3
Baseline (Conventional jet fuel)	89.0		

Appendix D

Minimum Selling Prices

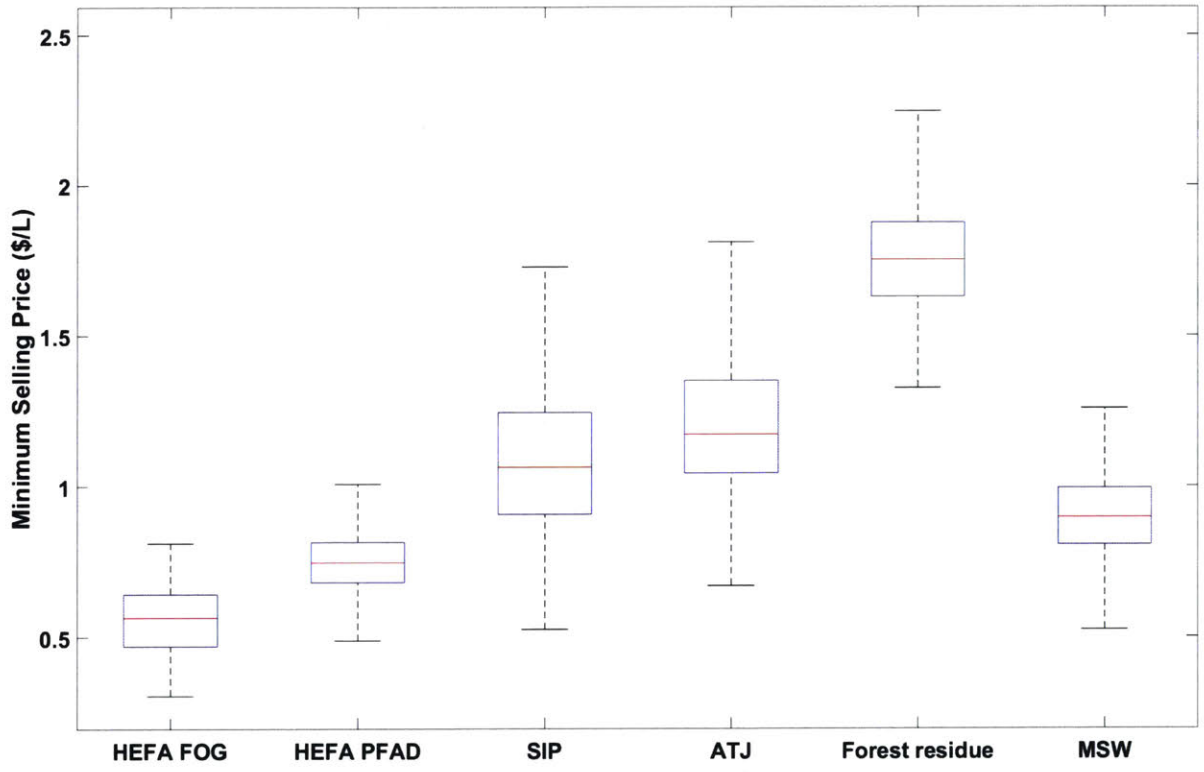

Figure D-1: Minimum selling prices of the renewable drop-in fuels assessed.

Appendix E

Composite Plot of Stochastic LCA Histograms

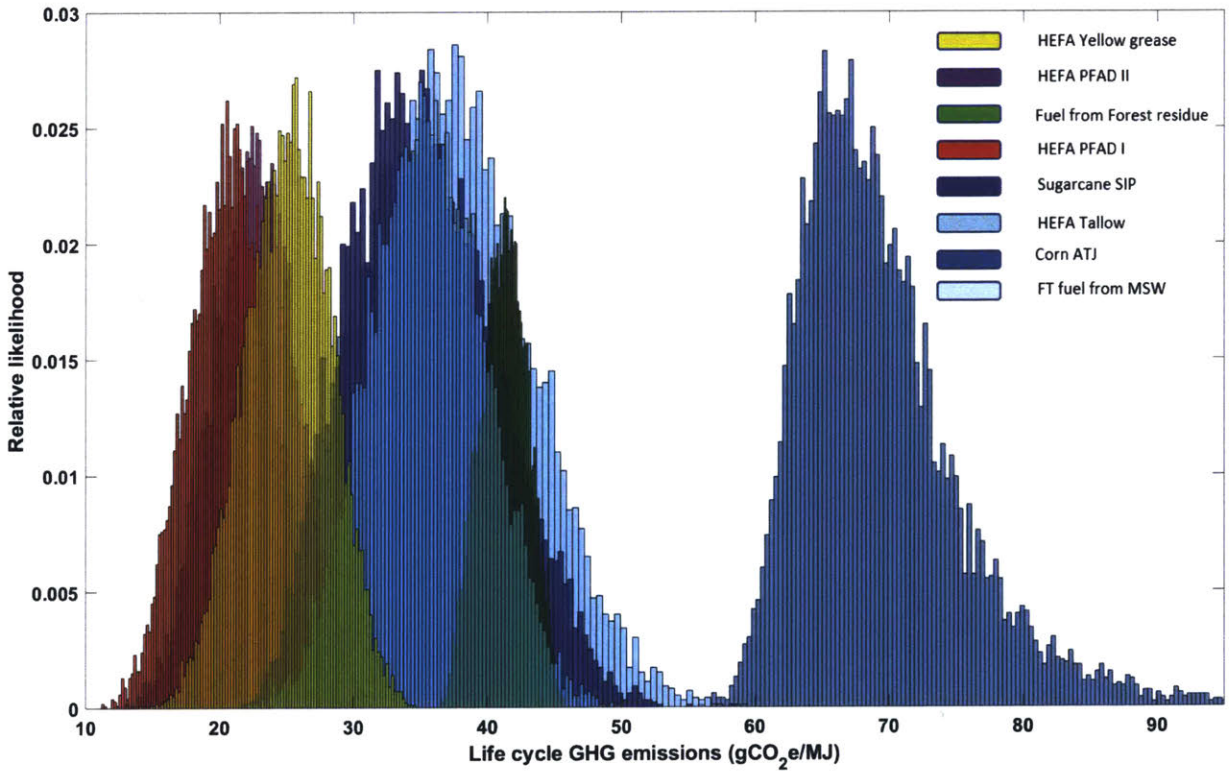

Figure E-1: Stochastic LCA histograms.

Bibliography

[1] I. E. Agency, *CO_2 Emissions from Fuel Combustion 2016*. OECD, 2016.

[2] D. S. Lee, D. W. Fahey, P. M. Forster, P. J. Newton, R. C. Wit, L. L. Lim, B. Owen, and R. Sausen, "Aviation and global climate change in the 21st century," *Atmospheric Environment*, vol. 43, no. 22-23, pp. 3520–3537, 2009.

[3] I.-I. A. T. Association *et al.*, "A global approach to reducing aviation emissions," *First stop: carbon-neutral growth from*, vol. 2020, 2009.

[4] ICAO, "Resolutions adopted at the 38th session of the assembly, provisional edition." https://www.iea.org/publications/freepublications/publication/CO2EmissionsfromFuelCombustion_

[5] ICAO, "International civil aviation organization (icao), 2016b. consolidated statement of continuing icao policies and practices related to environmental protection – global market-based measure (mbm) scheme." http://www.icao.int/environmentalprotection/Documents/Resolution_A39_3.pdf.

[6] ICAO, "International civil aviation organization (icao), 2017. what is corsia and how does it work?." http://www.icao.int/environmentalprotection/Pages/A39_CORSIA_FAQ2.aspx.

[7] M. D. Staples, R. Malina, P. Suresh, J. I. Hileman, and S. R. Barrett, "Aviation co2 emissions reductions from the use of alternative jet fuels," *Energy Policy*, vol. 114, pp. 342–354, 2018.

[8] M. D. Staples, R. Malina, H. Olcay, M. N. Pearlson, J. I. Hileman, A. Boies, and S. R. Barrett, "Lifecycle greenhouse gas footprint and minimum selling price of renewable diesel and jet fuel from fermentation and advanced fermentation production technologies," *Energy & Environmental Science*, vol. 7, no. 5, pp. 1545–1554, 2014.

[9] M. N. Pearlson, *A techno-economic and environmental assessment of hydroprocessed renewable distillate fuels*. PhD thesis, Massachusetts Institute of Technology, 2011.

[10] G. Seber, R. Malina, M. N. Pearlson, H. Olcay, J. I. Hileman, and S. R. Barrett, "Environmental and economic assessment of producing hydroprocessed jet and diesel fuel from waste oils and tallow," *Biomass and Bioenergy*, vol. 67, pp. 108–118, 2014.

[11] A. N. Laboratory. The greenhouse gases, regulated emissions, and energy use in transportation (GREET) computer model GREET1_2017. Argonne, IL; 2017.

[12] ICAO, "Icao document 10126, report of the eleventh meeting of the committee on aviation environmental protection, 2019."

[13] CAAFI, "Fuel qualification." http://caafi.org/focus_areas/fuel_qualification.html.

[14] ICAO. https://www.icao.int/environmental-protection/Pages/AltFuels_LifeCycleBox.aspx.

[15] U. S. D. of Agriculture. https://www.usda.gov/oce/climate_change/mitigation_technologies/USDAI

[16] U. S. D. of Agriculture. https://www.usda.gov/oce/reports/energy/2008Ethanol_June_final.pdf.

[17] M. Wang, J. Han, J. B. Dunn, H. Cai, and A. Elgowainy, "Well-to-wheels energy use and greenhouse gas emissions of ethanol from corn, sugarcane and cellulosic biomass for us use," *Environmental Research Letters*, vol. 7, no. 4, p. 045905, 2012.

[18] U. S. D. of Agriculture. https://www.usda.gov/oce/climate_change/mitigation_technologies/USDAI

[19] Food and A. O. of the United Nations. http://www.fao.org/docrep/007/y5376e/y5376e0a.htm.

[20] U. Br. http://www.unicadata.com.br/listagem.php?idMn=102.

[21] palmoilanalytics.com. http://www.palmoilanalytics.com/files/epos-final-59.pdf.

[22] S. S. Harsono, A. Prochnow, P. Grundmann, A. Hansen, and C. Hallmann, "Energy balances and greenhouse gas emissions of palm oil biodiesel in i ndonesia," *GCB Bioenergy*, vol. 4, no. 2, pp. 213–228, 2012.

[23] J. H. Schmidt, "Life assessment of rapeseed oil and palm oil. ph. d. thesis, part 3: Life cycle inventory of rapeseed oil," 2007.

[24] C. R., "Updates on the energy consumption of the beef tallow rendering process and the ratio of synthetic fertilizer nitrogen supplementing removed crop residue nitrogen in greet," 2017.

[25] P. Suresh, *Environmental and economic assessment of transportation fuels from municipal solid waste.* PhD thesis, Massachusetts Institute of Technology, 2016.

[26] M. Lariviere, "Methodology for allocating municipal solid waste to biogenic and non-biogenic energy," *Energy Information Administration, Office of Coal, Nuclear, Electric and Alternate Fuels. May. http://www. eia. doe. gov/cneaf/solar. renewables/page/mswaste/msw. pdf*, 2007.

[27] EPA, "United states environmental protection agency. (september 2015). waste reduction model (warm) version 13 (updated march 2015)." https://www.epa.gov/warm.

[28] J. Penman, D. Kruger, I. Galbally, T. Hiraishi, B. Nyenzi, S. Emmanuel, L. Buendia, R. Hoppaus, T. Martinsen, J. Meijer, *et al.*, "Good practice guidance and uncertainty management in national greenhouse gas inventories," 2000.

[29] EPA, "Advancing sustainable materials management: Facts and figures 2013," EPA530-R-15-002, 2015.

[30] S. A. Motycka, *Techno economic analysis of a plasma gasification biomass to liquids plant.* PhD thesis, The George Washington University, 2013.

[31] P. N. Pressley, T. N. Aziz, J. F. DeCarolis, M. A. Barlaz, F. He, F. Li, and A. Damgaard, "Municipal solid waste conversion to transportation fuels: a life-cycle estimation of global warming potential and energy consumption," *Journal of Cleaner Production*, vol. 70, pp. 145–153, 2014.

[32] P. N. Pressley, J. W. Levis, A. Damgaard, M. A. Barlaz, and J. F. DeCarolis, "Analysis of material recovery facilities for use in life-cycle assessment," *Waste Management*, vol. 35, pp. 307–317, 2015.

[33] A. C. Caputo and P. M. Pelagagge, "Rdf production plants: Ii economics and profitability," *Applied Thermal Engineering*, vol. 22, no. 4, pp. 439–448, 2002.

[34] A. M. Niziolek, O. Onel, M. F. Hasan, and C. A. Floudas, "Municipal solid waste to liquid transportation fuels–part ii: Process synthesis and global optimization strategies," *Computers & Chemical Engineering*, vol. 74, pp. 184–203, 2015.

[35] R. M. Swanson, A. Platon, J. Satrio, R. Brown, and D. D. Hsu, "Techno-economic analysis of biofuels production based on gasification," tech. rep., National Renewable Energy Lab.(NREL), Golden, CO (United States), 2010.

[36] D. Unruh, K. Pabst, and G. Schaub, "Fischer- tropsch synfuels from biomass: maximizing carbon efficiency and hydrocarbon yield," *Energy & Fuels*, vol. 24, no. 4, pp. 2634–2641, 2010.

[37] EPA, "'"combustion" in documentation for greenhouse gas emission and energy factors used in the waste reduction model (warm) version 13." https://www3.epa.gov/warm/pdfs/WARM_Documentation.pdf.

[38] R. Williams, B. Jenkins, and D. Nguyen, "Solid waste conversion: A review and database of current and emerging technologies," *Final report, Department of Biological and Agricultural Engineering, University of California, Davis*, 2003.

[39] B. M. Güell, M. Bugge, R. S. Kempegowda, A. George, and S. M. Paap, "Benchmark of conversion and production technologies for synthetic biofuels for aviation," *SINTEF Energy Research, Norway*, 2012.

[40] G. Doka, "Life cycle inventories of waste treatment services," *Final report ecoinvent*, no. 13, 2003.

[41] H. Eggleston, L. Buendia, K. Miwa, T. Ngara, and K. Tanabe, "Intergovernmental panel on climate change. 2006 ipcc guidelines for national greenhouse gas inventories—vol. 4, agriculture, forestry and other land use," *Prepared by the National Greenhouse Gas Inventories Programme IGES, Japan*, 2006.

[42] J. Z. Wang, *Quantitative policy analysis for aviation biofuel production technologies*. PhD thesis, Massachusetts Institute of Technology, 2019.

[43] S. J. Bann, *A stochastic techno-economic comparison of alternative jet fuel production pathways*. PhD thesis, Massachusetts Institute of Technology, 2017.

[44] EIA, "Petroleum and other liquids; spot prices." https://www.eia.gov/dnav/pet/petprispts1m.htm.

[45] ICAO, "A marginal abatement cost curve model for the uk aviaition sector." https://www.icao.int/environmental-protection/Documents/ActionPlan/UK_AbatementModel_en.pdf.

[46] https://media.nature.com/original/nature-assets/nclimate/journal/v6/n4/extref/nclimate2865-s1.pdf.

[47] J. Bosch, S. D. JONG, D. HOEFNAGELS, and D. R. SLADE, "Aviation biofuels: strategically important, technically achievable, tough to deliver," *Grantham Institute Briefing Paper No*, vol. 23, 2017.

[48] IATA, "Fact sheet: Fuel [online]." https://www.iata.org/pressroom/facts_figures/fact_sheets/Docum sheet-fuel.pdf.

[49] R. Mohsin, T. Kumar, Z. Majid, I. Kumar, and A. Wash, "Assessment of usage of biofuel in aviation industry in malaysia," *Chemical Engineering Transactions*, vol. 56, pp. 277–282, 2017.

[50] EU. https://ec.europa.eu/energy/en/topics/renewable-energy/biofuels/biofuels-aviation.

[51] H. M. Noh, A. Benito, and G. Alonso, "Study of the current incentive rules and mechanisms to promote biofuel use in the eu and their possible application to the civil aviation sector," *Transportation Research Part D: Transport and Environment*, vol. 46, pp. 298–316, 2016.

[52] "How corn is processed to make ethanol." https://www.e-education.psu.edu/egee439/node/673.

[53] M. Pearlson, C. Wollersheim, and J. Hileman, "A techno-economic review of hydroprocessed renewable esters and fatty acids for jet fuel production," *Biofuels, Bioproducts and Biorefining*, vol. 7, no. 1, pp. 89–96, 2013.

[54] A. Steynberg and M. Dry, "Chemical concepts used for engineering purposes," in *Fischer-Tropsch Technology*, vol. 152, pp. 196–257, Elsevier Amsterdam, Boston, 2004.

[55] "Process for the production of isoparaffins." https://patents.google.com/patent/US5292983.

[56] "Microreactor." https://en.wikipedia.org/wiki/Microreactor.

[57] L. C. Almeida, O. Sanz, J. D'olhaberriague, S. Yunes, and M. Montes, "Microchannel reactor for fischer–tropsch synthesis: Adaptation of a commercial unit for testing microchannel blocks," *Fuel*, vol. 110, pp. 171–177, 2013.

[58] W. Ehrfeld, V. Hessel, and H. Löwe, "Microreactors: New technology for modern chemistry 2000," 2005.